Carborane Complexes of Ruthenium: Studies on the Chemistry of the $Ru(CO)_2(\eta^5\text{-}7,8\text{-}C_2B_9H_{11})$ Fragment†

Stephen Anderson, Donald F. Mullica, Eric L. Sappenfield, and F. Gordon A. Stone*

Department of Chemistry, Baylor University, Waco, TX 76798-7348

Received December 7, 1995⊗

Treatment of $[Ru(CO)_3(\eta^5\text{-}7,8\text{-}C_2B_9H_{11})]$ (**1**) with Me_3NO in THF (tetrahydrofuran) affords $[Ru(CO)_2(NMe_3)(\eta^5\text{-}7,8\text{-}C_2B_9H_{11})]$ (**3b**), while the salt $[NEt_4][RuI(CO)_2(\eta^5\text{-}7,8\text{-}C_2B_9H_{11})]$ (**2**) reacts with NCMe in the presence of $AgBF_4$ to give $[Ru(CO)_2(NCMe)(\eta^5\text{-}7,8\text{-}C_2B_9H_{11})]$ (**3c**). Related complexes $[Ru(CO)_2(L)(\eta^5\text{-}7,8\text{-}C_2B_9H_{11})]$ (L = $CNBu^t$ (**3d**), PPh_3 (**3e**)) are obtained by displacement of THF from $[Ru(CO)_2(THF)(\eta^5\text{-}7,8\text{-}C_2B_9H_{11})]$ (**3a**) with $CNBu^t$ and PPh_3, respectively. Alkenes and **3a** afford the complexes $[Ru(CO)_2(alkene)(\eta^5\text{-}7,8\text{-}C_2B_9H_{11})]$ (alkene = C_2H_4 (**4a**), $MeCH{=}CH_2$ (**4b**), $Me_3SiCH{=}CH_2$ (**4c**), and C_7H_{10} (norbornene) (**4d**)), whereas alkynes RC≡CR (R = Me, Ph) give the species $[Ru(CO)_2(RC{\equiv}CR)(\eta^5\text{-}7,8\text{-}C_2B_9H_{11})]$ (R = Me (**5a**), Ph (**5b**)). The reaction of complex **5a** with $K[BH(CHMeEt)_3]$, in Et_2O solution, followed by addition of 18-crown-6, gives the salt $[K(18\text{-crown-6})][Ru\{C(Me){=}C(H)Me\}(CO)_2(\eta^5\text{-}7,8\text{-}C_2B_9H_{11})]$ (**6**), while PPh_3 in CH_2Cl_2 affords the ylide complex $[Ru\{C(Me){=}C(Me)PPh_3\}(CO)_2(\eta^5\text{-}7,8\text{-}C_2B_9H_{11})]$ (**7**). Reactions between **3a** and the alkynes RC≡CH (R = Bu^t, $SiMe_3$) yield a variety of products, in all of which the carborane ligand adopts a nonspectator role. Complex **3a** and 1 mol equiv of $Bu^tC{\equiv}CH$ gives a mixture of isomers $[Ru(CO)_2(\eta^2{:}\eta^5\text{-}9\text{-}C(H){=}C(H)Bu^t\text{-}7,8\text{-}C_2B_9H_{10})]$ (**8a**) and $[Ru(CO)_2(\eta^2{:}\eta^5\text{-}10\text{-}C(H){=}C(H)Bu^t\text{-}7,8\text{-}C_2B_9H_{10})]$ (**8b**). An X-ray diffraction study on **8a** revealed that the ruthenium atom is η^5-coordinated by the open CCBBB face of the *nido*-C_2B_9 cage and by the C=C bond of the $BCH{=}C(H)Bu^t$ group. The reaction between **3a** and 1 mol equiv of $Me_3SiC{\equiv}CH$ is more complex due to $SiMe_3$ group cleavage. Isomeric mixtures of $[Ru(CO)_2(\eta^2{:}\eta^5\text{-}9\text{-}C(H){=}C(H)R\text{-}7,8\text{-}C_2B_9H_{10})]$ (R = H (**9a**), $SiMe_3$ (**10a**)) and $[Ru(CO)_2(\eta^2{:}\eta^5\text{-}10\text{-}C(H){=}C(H)R\text{-}7,8\text{-}C_2B_9H_{10})]$ (R = H (**9b**), $SiMe_3$ (**10b**)) are obtained. Addition of PMe_2Ph in heptane to **9b** gives $[Ru(CO)_2(\sigma,\eta^5\text{-}10\text{-}C(H)(PMe_2Ph)\text{-}CH_2\text{-}7,8\text{-}C_2B_9H_{10})]$ (**11b**), the ylide structure of which was confirmed by X-ray crystallography. The $Ru(CO)_2$ fragment is linked to the *nido*-C_2B_9 cage system by η^5 bonding to the CCBBB face and by a $Ru{-}CH_2$ σ-bond to the $CH_2C(H)(PMe_2Ph)B$ fragment. Reactions between **3a** and RC≡CH, employing an excess of the latter, give the compounds $[Ru(CO)_2\{\eta^2{:}\eta^5\text{-}9\text{-}C(H){=}C(H)R\text{-}10,11\text{-}[C(H){=}C(H)R]_2\text{-}7,8\text{-}C_2B_9H_8\}]$ (R = Bu^t (**12a**), $SiMe_3$ (**12b**)) in which all boron atoms in the open CCBBB face of the cage bonded to the ruthenium carry C(H)=C(H)R substituents. Treatment of the complexes **12** with PMe_3 yields respectively $[Ru(CO)_2(PMe_3)\{\eta^5\text{-}9,10,11\text{-}[C(H){=}C(H)Bu^t]_3\text{-}7,8\text{-}C_2B_9H_8\}]$ (**13**) and $[Ru(CO)_2\{\sigma,\eta^5\text{-}9\text{-}C(H)(PMe_3)C(H)SiMe_3\text{-}10,11\text{-}[C(H){=}C(H)SiMe_3]_2\text{-}7,8\text{-}C_2B_9H_8\}]$ (**14**). The structure of **13** was established by X-ray diffraction. The Ru atom is coordinated by a PMe_3 molecule and the two CO groups and by the *nido*-9,10,11-$[C(H){=}C(H)Bu^t]_3$-7,8-$C_2B_9H_8$ cage. All boron atoms in the pentagonal CCBBB ring ligating the metal carry $C(H){=}C(H)Bu^t$ substituents. In addition to X-ray crystal structure determinations, NMR data for the new complexes are reported and discussed in relation to their structures.

Downloaded by CARLI CONSORTIUM on June 30, 2009
Published on March 19, 1996 on http://pubs.acs.org | doi: 10.1021/om950934+

Introduction

We have recently reported a convenient high-yield synthesis of the mononuclear ruthenium complex $[Ru(CO)_3(\eta^5\text{-}7,8\text{-}C_2B_9H_{11})]$ (**1**),[1] a molecule likely to have considerable potential as a source of a variety of species containing the $Ru(CO)_2(\eta^5\text{-}7,8\text{-}C_2B_9H_{11})$ fragment. The latter group is isolobal with the well-known cyclopentadienyldicarbonylmetal moieties $[Ru(CO)_2(\eta^5\text{-}C_5H_5)]^-$ and $Mn(CO)_2(\eta^5\text{-}C_5H_5)$, which are known to play an extensive role in organometallic chemistry. Thus, a detailed study of the chemistry of **1** and its derivatives is warranted. In this paper we describe the synthesis and reactivity of several complexes of the type $[Ru(CO)_2(L)(\eta^5\text{-}7,8\text{-}C_2B_9H_{11})]$ (L = donor ligand), as well as some

* To whom correspondence should be addressed.

† In the compounds described in this paper, ruthenium atoms and *nido*-C_2B_9 cages form *closo*-1,2-dicarba-3-ruthenadodecaborane structures. However, use of this numbering scheme leads to a complicated nomenclature for some of the metal complexes reported. Following precedent (Mullica, D. F.; Sappenfield, E. L.; Stone, F. G. A.; Woollam, S. F. *Organometallics* **1994**, *13*, 157), therefore, we treat the cage as a *nido* 11-vertex ligand with numbering as for an icosahedron from which the 12th vertex has been removed. This has the added convenience of relating the metal carborane complexes to isolobal species with η^5-C_5H_5 ligands.

⊗ Abstract published in *Advance ACS Abstracts,* February 15, 1996.

(1) Anderson, S.; Mullica, D. F.; Sappenfield, E. L.; Stone, F. G. A. *Organometallics* **1995**, *14*, 3516.

0276-7333/96/2315-1676$12.00/0 © 1996 American Chemical Society

Table 1. Analytical and Physical Data

comp	color	yield/%	ν_{max}(CO)[a]/cm^{-1}	anal./%[b] C	anal./%[b] H
[Ru(CO)$_2$(NMe$_3$)(η^5-7,8-C$_2$B$_9$H$_{11}$)] (**3b**)	yellow	73	2047 s, 1994 s	24.3[c] (24.1)	6.0 (5.8)
[Ru(CO)$_2$(NCMe)(η^5-7,8-C$_2$B$_9$H$_{11}$)] (**3c**)	yellow	66	2064 s, 2013 s	21.9[d] (21.8)	4.5 (4.3)
[Ru(CO)$_2$(CNBu^t)(η^5-7,8-C$_2$B$_9$H$_{11}$)] (**3d**)	yellow	74	2192 s,[e] 2067 s, 2023 s	28.3[f] (29.0)	5.4 (5.4)
[Ru(CO)$_2$(PPh$_3$)(η^5-7,8-C$_2$B$_9$H$_{11}$)] (**3e**)	yellow	69	2052 s, 2006 s	47.3 (47.9)	4.5 (4.8)
[Ru(CO)$_2$(C$_2$H$_4$)(η^5-7,8-C$_2$B$_9$H$_{11}$)] (**4a**)	yellow	79	2076 s, 2030 s	22.0 (22.7)	4.4 (4.8)
[Ru(CO)$_2$(MeCH=CH$_2$)(η^5-7,8-C$_2$B$_9$H$_{11}$)] (**4b**)	yellow	74	2070 s, 2024 s	25.6 (25.4)	5.3 (5.2)
[Ru(CO)$_2$(Me$_3$SiCH=CH$_2$)(η^5-7,8-C$_2$B$_9$H$_{11}$)] (**4c**)	yellow	77	2070 s, 2024 s	28.2 (27.7)	6.3 (6.0)
[Ru(CO)$_2$(C$_7$H$_{10}$)(η^5-7,8-C$_2$B$_9$H$_{11}$)] (**4d**)	white	89	2066 s, 2020 s	34.9 (34.4)	5.8 (5.5)
[Ru(CO)$_2$(MeC≡CMe)(η^5-7,8-C$_2$B$_9$H$_{11}$)] (**5a**)	yellow	72	2066 s, 2019 s	27.5 (28.0)	5.2 (5.0)
[Ru(CO)$_2$(PhC≡CPh)(η^5-7,8-C$_2$B$_9$H$_{11}$)] (**5b**)	yellow	64	2076 s, 2032 s	41.8[g] (41.3)	4.3 (4.2)
[K(18-crown-6)][Ru{C(Me)=C(H)Me}(CO)$_2$(η^5-7,8-C$_2$B$_9$H$_{11}$)] (**6**)	red	69	2004 s, 1942 s	35.5[h] (35.7)	6.4 (6.3)
[Ru{C(Me)=C(Me)PPh$_3$}(CO)$_2$(η^5-7,8-C$_2$B$_9$H$_{11}$)] (**7**)	yellow	62	2020 s, 1964 s	48.4[h] (49.1)	4.9 (5.1)
[Ru(CO)$_2$(η^2:η^5-*n*-C(H)=C(H)Bu^t-7,8-C$_2$B$_9$H$_{10}$)] (**8**)[i]	yellow	66	2050 s, 2004 s	32.4 (32.3)	5.7 (5.7)
[Ru(CO)$_2$(η^2:η^5-*n*-C(H)=CH$_2$-7,8-C$_2$B$_9$H$_{10}$)] (**9**)[i,j]	yellow	69	2054 s, 2005 s	24.4 (22.8)	4.3 (4.2)
[Ru(CO)$_2$(η^2:η^5-*n*-C(H)=C(H)SiMe$_3$-7,8-C$_2$B$_9$H$_{10}$)] (**10**)[i,j]	yellow	40	2052 s, 2002 s		
[Ru(CO)$_2$(σ,η^5-10-C(H)(PMe$_2$Ph)CH$_2$-7,8-C$_2$B$_9$H$_{10}$)] (**11b**)	white	60	1998 s, 1934 s	35.4[b] (35.1)	5.1 (5.1)
[Ru(CO)$_2$\{η^2:η^5-9-C(H)=C(H)Bu^t-10,11-[C(H)=C(H)Bu^t]$_2$-7,8-C$_2$B$_9$H$_8$\}] (**12a**)	yellow	56	2048 s, 2000 s	44.4[g] (44.5)	7.3 (7.0)
[Ru(CO)$_2$\{η^2:η^5-9-C(H)=C(H)SiMe$_3$-10,11[C(H)=C(H)SiMe$_3$]$_2$-7,8-C$_2$B$_9$H$_8$\}] (**12b**)	yellow	51	2052 s, 2004 s	37.9[h] (37.4)	6.9 (6.8)
[Ru(CO)$_2$(PMe$_3$)\{η^5-9,10,11-[C(H)=C(H)Bu^t]$_3$-7,8-C$_2$B$_9$H$_8$\}] (**13**)	white	69	2046 s, 2000 s	49.1 (49.1)	8.2 (8.2)
[Ru(CO)$_2$\{σ,η^5-9-C(H)(PMe$_3$)C(H)SiMe$_3$-10,11-[C(H)=C(H)SiMe$_3$]$_2$-7,8-C$_2$B$_9$H$_8$\}] (**14**)	yellow	71	2002 s, 1944 s	39.2 (40.0)	7.0 (7.6)

[a] Measured in CH_2Cl_2. A medium-intensity broad band observed at ca. 2550 cm^{-1} in the spectra of all the compounds is due to B—H absorptions. [b] Calculated values are given in parentheses. [c] N, 4.1 (4.0). [d] N, 4.2 (4.2). [e] ν_{max}(NC). [f] N, 3.4 (3.8). [g] Crystallizes with a molecule of CH_2Cl_2. [h] Crystallizes with 0.5 of a molecule of CH_2Cl_2. [i] n = 9 or 10; complexes are formed as isomeric mixtures with the cage substituent attached to a B atom which is either α or β to the carbons in the open CCBBB face ligating the ruthenium (see text). [j] **9** and **10** form as a mixture and could not be obtained entirely free of each other; hence, satisfactory microanalytical data were not obtained (see text).

Downloaded by CARLI CONSORTIUM on June 30, 2009
Published on March 19, 1996 on http://pubs.acs.org | doi: 10.1021/om950934+

novel products obtained from reactions involving the alkynes RC≡CH (R = Bu^t or SiMe$_3$).

Results and Discussion

We have previously shown that the reaction between complex **1** and [NEt$_4$]I in THF at reflux temperatures gives the salt [NEt$_4$][RuI(CO)$_2$(η^5-7,8-C$_2$B$_9$H$_{11}$)] (**2**) and that treatment of the latter with AgBF$_4$ in THF (tetrahydrofuran) affords [Ru(CO)$_2$(THF)(η^5-7,8-C$_2$B$_9$H$_{11}$)] (**3a**), AgI, and [NEt$_4$][BF$_4$].[1] Extraction of this mixture of products with CH_2Cl_2 yields solutions of **3a** in essentially quantitative yield. As described below, these CH_2Cl_2 solutions may be used for further preparative work without isolation of **3a**. However, since the intermediacy of **2** is required in this synthesis of the THF complex, it seemed desirable to attempt to obtain **3a** directly from **1**. Since Me$_3$NO is known to remove CO ligands as CO_2, treatment of THF solutions of **1** with the amine oxide was investigated. The product obtained, however, was [Ru(CO)$_2$(NMe$_3$)(η^5-7,8-C$_2$B$_9$H$_{11}$)] (**3b**), rather than the desired THF complex **3a**. Moreover, compound **3b** proved to be relatively stable, and it was not possible to replace the NMe$_3$ ligand by other donor molecules in reactions at ambient temperatures. Data fully characterizing **3b** are given in Tables 1 and 2.

The reaction between **2** and AgBF$_4$ in NCMe was next investigated, and the complex [Ru(CO)$_2$(NCMe)(η^5-7,8-C$_2$B$_9$H$_{11}$)] (**3c**) was thereby isolated in good yield. Whereas **3a** forms rapidly from **2** and AgBF$_4$ in THF, the synthesis of **3c** requires *ca.* 1 h for completion. The IR spectrum of **3c**, measured in CH_2Cl_2, showed two CO stretching bands at 2064 and 2013 cm^{-1} (Table 1). The NMR spectra (Table 2) revealed resonances for the ligated NCMe molecule at δ 2.35 in the ^{1}H spectrum and at δ 142.5 (N*C*Me) and 4.3 (Me) in the ^{13}C{^{1}H} spectrum. There was no evidence for dissociation of the NCMe ligand of **3c** in nondonor solvents. In contrast,

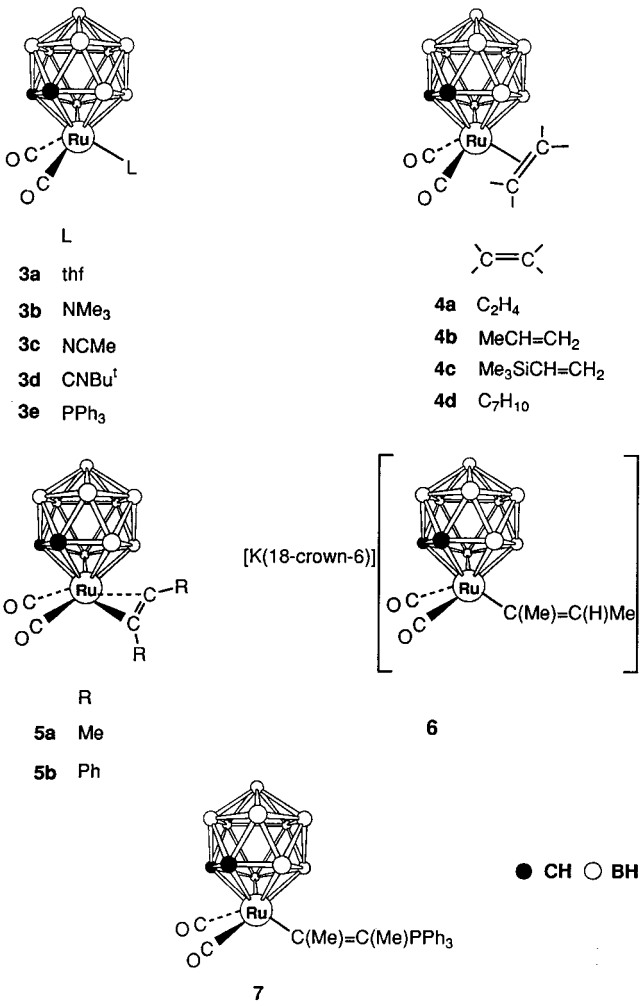

Table 2. Hydrogen-1, Carbon-13, and Boron-11 NMR Data[a]

compd	^{1}H/δ[b]	^{13}C/δ[c]	^{11}B/δ[d]
3b	2.80 (s, 9 H, Me), 2.98 (s, 2 H, cage CH)	196.3 (CO), 59.3 (Me), 50.6 (cage CH)	2.4 (1 B), −7.0 (2 B), −10.1 (3 B), −19.8 (3 B)
3c	2.35 (s, 3 H, Me), 3.23 (s, 2 H, cage CH)	193.8 (CO), 142.5 (N*C*Me), 48.9 (cage CH), 4.3 (Me)	4.3 (1 B), −7.0 (2 B), −8.3 (2 B), −10.1 (1 B), −18.0 (1 B), −20.9 (2 B)
3d	1.55 (s, 9 H, Me), 3.20 (s, 2 H, cage CH)	193.1 (CO), 134.2 (br, *C*NBu^t), 60.3 (*C*Me$_3$), 44.1 (cage CH), 30.5 (C*Me*$_3$)	4.7 (1 B), −5.6 (1 B), −6.7 (2 B), −9.4 (2 B), −19.7 (3 B)
3e	2.18 (s, 2 H, cage CH), 7.5 (m, 15 H, Ph)	196.5 (CO, d, J(PC) = 15), 133.3−129.8 (Ph), 48.0 (cage CH)	4.0 (1 B), −4.5 (1 B), −6.3 (3 B), −9.2 (2 B), −19.4 (2 B)
4a	2.76 (s, 2 H, cage CH), 3.80 (s, 4 H, C_2H_4)	195.9 (CO), 64.6 (C═C), 51.3 (cage CH)	6.1 (1 B), −2.9 (1 B), −4.8 (2 B), −8.8 (2 B), −17.7 (3 B)
4b	2.05 (d, 3 H, Me, J(HH) = 6.0), 2.68, 2.86 (s × 2, 2 H, cage CH), 3.65 (d, 1 H, ═CH$_2$, J(HH) = 8), 3.82 (d, 1 H, ═CH$_2$, J(HH) = 14), 4.78 (m, 1 H, ═CH)	196.2 (CO), 90.6, 66.6 (C═C), 51.4, 51.0 (cage CH), 21.8 (Me)	5.7 (1 B), −4.1 (1 B), −5.2 (2 B), −8.9 (2 B), −18.1 (3 B)
4c	0.26 (s, 9 H, SiMe$_3$), 2.49, 2.95 (s × 2, 2 H, cage CH), 3.44 (d of d, 1 H, ═CH, J(HH) = 17, 12), 3.97 (d of d, 1 H, ═CH$_2$, J(HH) = 17, 1), 4.08 (d of d, 1 H, ═CH$_2$, J(HH) = 12, 1)	196.7, 196.3 (CO), 80.8, 71.1 (C═C), 50.1 (br, cage CH), −0.74 (SiMe$_3$)	6.2 (1 B), −3.4 (1 B), −4.2 (1 B), −5.1 (1 B), −8.5 (2 B), −17.7 (3 B)
4d	0.75, 1.02 (m × 2, 2 H, CH$_2$), 1.12, 1.80 (m × 2, 4 H, CH$_2$), 2.58 (s, 2 H, cage CH), 3.11 (s, 2 H, CH), 4.35 (s, 2 H, ═CH)	197.2 (CO), 86.6 (C═C), 52.6 (cage (CH), 41.8, 37.9, 25.6 (C_7H_{10})	4.7 (1 B), −2.9 (1 B), −4.9 (2 B), −9.4 (2 B), −17.0 (2 B), −19.0 (1 B)
5a	2.44 (s, 6 H, Me), 2.68 (s, 2 H, cage CH)	195.4 (CO), 63.8 (C≡C), 53.0 (cage CH), 10.2 (Me)	4.8 (1 B), −5.4 (3 B), −8.6 (2 B), −17.2 (1 B), −18.8 (2 B)
5b	2.85 (s, 2 H, cage CH), 7.55 (m, 10 H, Ph)	195.0 (CO), 132.2−123.4 (Ph), 80.3 (C≡C), 52.9 (cage CH)	6.5 (1 B), −4.1 (3 B), −7.1 (2 B), −16.2 (1 B), −18.4 (2 B)
6	1.65 (d of q br, 3 H, Me, J(HH) = 7, 1.5), 2.26 (m, 3 H, Me, J(HH) = 1.5), 2.32 (s, 2 H, cage CH), 3.63 (s, 24 H, 18-crown-6), 5.95 (q of q, 1 H, CH, J(HH) = 7, 1.5)	201.8 (CO), 149.3, 126.2 (C═C), 70.5 (18-crown-6), 43.1 (cage CH), 38.8, 20.4 (Me)	−6.3 (1 B), −8.2 (1 B), −10.8 (2 B), −12.7 (2 B), −20.5 (1 B), −22.8 (2 B)
7	2.10 (m × 2, 3 H, CMe, J(PH) = 15), 2.46 (m, 3 H, CMe), 2.54 (s, 2 H, cage CH), 7.67 (m, 15 H, PPh$_3$)	199.0 (CO), 134.3−130.0 (Ph), 122.4 (d, *C*Me, J(PC) = 82), 107.5 (d, *C*Me, J(PC) = 51), 43.3 (d, Me, J(PC) = 19), 42.0 (cage CH), 29.1 (d, Me, J(PC) = 24)	−3.0 (1 B), −7.4 (1 B), −9.2 (2 B), −11.1 (2 B), −19.9 (1 B), −21.9 (2 B)
8a	1.33 (s, 9 H, Bu^t), 1.84, 4.16 (s × 2, 2 H, cage CH), 4.76 (d, 1 H, ═CH, J(HH) = 14), 4.86 (d, 1 H, ═CH, J(HH) = 14)	196.2, 194.4 (CO), 110.0 (═*C*HBu^t), 86.5 (vbr, ═CHB), 57.7 (cage CH), 52.5 (*C*Me$_3$), 37.4 (vbr, cage CH), 31.2 (C*Me*$_3$)	8.1 (1 B, BC═C), 6.4 (1 B), 5.5 (1 B), 3.0 (1 B), −13.7 (1 B), −14.6 (1 B), −17.2 (1 B), −19.5 (1 B), −21.4 (1 B)
8b	1.32 (s, 9 H, Bu^t) 3.39, 3.94 (s × 2, 2 H, cage CH), 4.90 (d, 1 H, ═CH, J(HH) = 13), 5.08 (d, 1 H, ═CH, J(HH) = 13)	195.2, 193.4 (CO), 107.5 (═*C*HBu^t), 86.5 (vbr, ═CHB), 52.5 (*C*Me$_3$), 37.4 (vbr, cage CH), 31.6 (C*Me*$_3$)	17.8 (1 B, BC═C), 2.3 (1 B), −7.1 (1 B), −7.6 (1 B), −9.3 (1 B), −12.3 (1 B), −15.8 (2 B), −23.8 (1 B)
9a	1.72, 4.20 (s × 2, 2 H, cage CH), 3.36 (d, 1 H, ═CH$_2$, J(HH) = 14), 4.35 (d br, 1 H, ═CH$_2$, J(HH) = 10), 4.96 (d of d, 1 H, ═CHB, J(HH) = 14, 10)	197.0, 194.1 (CO), 63.2 (═CH$_2$), 59.0, 38.6 (cage CH)[e]	9.4 (1 B, BC═C), 6.5 (1 B), 5.3 (1 B), 3.0 (1 B), −13.3 (1 B), −14.4 (1 B), −17.0 (1 B), −19.1 (1 B), −21.3 (1 B)
9b	3.52, 3.98 (s × 2, 2 H, cage CH), 3.72 (d, 1 H, ═CH$_2$, J(HH) = 13), 4.41 (m br, 1 H, ═CH$_2$), 5.01 (d of d, 1 H, ═CHB, J(HH) = 13, 10)	194.6, 191.8 (CO), 59.1 (═CH$_2$), 38.6 (br, cage CH)[e]	18.9 (1 B, BC═C), 2.2 (1 B), −6.8 (1 B), −7.3 (1 B), −9.4 (1 B), −12.6 (1 B), −15.1 (1 B), −15.8 (1 B), −23.2 (1 B)
10a	0.28 (s, 9 H, SiMe$_3$), 1.80, 4.17 (s × 2, 2 H, cage CH), 3.52 (d, 1 H, ═CH, J(HH) = 16), 5.00 (d, 1 H, ═CH, J(HH) = 16)	198.1, 194.1 (CO), 98.5 (vbr, ═CHB), 79.4 (═*C*HSiMe$_3$), 58.3, 38.3 (br, cage CH), −0.6 (SiMe$_3$)	10.2 (1 B, BC═C), 6.5 (1 B), 5.8 (1 B), 3.2 (1 B), −13.4 (1 B), −14.5 (1 B), −16.8 (1 B), −19.2 (1 B), −21.4 (1 B)
10b	0.32 (s, 9 H, SiMe$_3$), 3.47, 3.96 (s × 2, 2 H, cage CH), 3.87 (d, 1 H, ═CH, J(HH) = 15), 5.06 (d, 1 H, ═CH, J(HH) = 15)	195.2, 192.7 (CO), 98.5 (vbr, ═CHB), 75.8 (═*C*HSiMe$_3$), 38.3 (br, cage CH), −0.6 (SiMe$_3$)	20.0 (1 B, BC═C), 2.8 (1 B), −6.7 (1 B), −7.4 (1 B), −9.4 (1 B), −12.4 (1 B), −15.0 (1 B), −15.6 (1 B), −23.4 (1 B)
11b	1.34 (d of d, 1 H, CH$_2$, J(HH) = 9, 7), 1.40 (d of d, 1 H, CH$_2$, J(HH) = 9, 8), 1.64 (d of d, 1 H, CH, J(HH) = 8, J(PH) = 3), 1.79 (d, 3 H, PMe, J(PH) = 13), 1.90 (d, 3 H, PMe, J(PH) = 15), 2.98, 3.38 (s × 2, 2 H, cage CH), 7.69 (m, 5 H, PPh)	199.7, 197.7 (CO), 133.9−126.5 (Ph), 123.2 (d, J(PC) = 36, C^1(Ph)), 44.5 38.8 (cage CH), 7.9, 5.5 (d × 2, PMe$_2$, J(PC = 54, 57), 1.0 (CH$_2$)[e]	−6.4 (1 B, BCP), −8.5 (1 B), −10.4 (1 B), −12.1 (1 B), −13.8 (1 B), −16.5 (1 B), −18.6 (1 B), −20.1 (1 B), −27.0 (1 B)
12a	1.09, 1.16, 1.21 (s × 3, 27 H, Bu^t) 2.33, 4.21 (s × 2, 2 H, cage CH), 4.85 (d, 1 H, ═CH, J(HH) = 12), 5.45 (d, 1 H, ═CH, J(HH) = 12), 5.55 (d, 1 H, ═CH, J(HH) = 16), 5.78 (d, 1 H, ═CH, J(HH) = 16), 5.80 (d, 1 H, ═CH, J(HH) = 16), 5.95 (d, 1 H, ═CH, J(HH) = 16)	195.8, 193.6 (CO), 148.9, 145.9 (═*C*HBu^t), 130.2 (vbr, ═CHB), 107.0 (═*C*HBu^t), 84.8 (vbr, ═CHB), 59.9, 40.7 (cage CH), 34.0, 32.1, 30.9 (C*Me*$_3$)[f]	15.4 (1 B, BC═C), 10.9 (1 B, B−C), 5.6 (1 B), 2.4 (1 B), −2.5 (1 B, BC═C), −14.1 (br, 2 B), −18.0 (1 B), −19.6 (1 B)

Downloaded by CARLI CONSORTIUM on June 30, 2009
Published on March 19, 1996 on http://pubs.acs.org | doi: 10.1021/om950934+

Table 2 (Continued)

compd	^{1}H/δ[b]	^{13}C/δ	^{11}B/δ[d]
12b	0.25 (s, 27 H, $SiMe_3$), 1.71, 4.43 (s × 2, 2 H, CH), 3.56 (d, 1 H, =CH, J(HH) = 16), 5.10 (d, 1 H, =CH, J(HH) = 16), 6.10 (d, 1 H, =CH, J(HH) = 21), 6.18 (d, 1 H, =CH, J(HH) = 21), 6.47 (d, 1 H, =CH, J(HH) = 21), 6.75 (d, 1 H, =CH, J(HH) = 21)	195.4, 194.6 (CO), 151.4 (vbr, =CHB), 141.3, 139.5 (=*C*HSiMe_3), 101.9 (vbr, =CHB), 79.8 (=*C*HSiMe_3), 55.8, 35.4 (cage CH), −0.5, −1.28, −1.31 ($SiMe_3$)	17.5 (1 B, BC=C), 10.3 (1 B, BC=C), 4.3 (1 B), 3.6 (1 B), −2.0 (1 B, B−C), −14.4 (1 B), −16.9 (1 B), −19.1 (1 B), −22.5 (1 B)
13	1.04 (s, 18, Bu^t), 1.10 (s, 9 H, Bu^t), 1.67 (d, 9 H, PMe_3, J(PH) = 10), 2.88 (s, 2 H, cage CH), 5.41 (d, 2 H, =CH, J(HH) = 16), 5.53 (d, 2 H, =CH, J(HH) = 16), 5.69 (d, 1 H, =CH, J(HH) = 16), 6.28 (d, 1 H, =CH, J(HH) = 16)	196.6 (CO, d, J(PC) = 17), 150.6 (1 C, =*C*HBu^t), 143.6 (2 C, =*C*HBu^t), 43.4 (cage CH), 31.6, 30.9 (C*Me*$_3$), 17.8 (d, PMe_3, J(PC) = 32)[e,f]	9.0 (1 B, BC=C) 1.0 (2 B, BC=C), 0.4 (1 B), −4.3 (2 B), −18.9 (3 B)
14	0.00, 0.03, 0.19 (s × 3, 27 H, $SiMe_3$), 1.54 (d, 1 H, C*H*$SiMe_3$, J(HH) = 15), 1.63 (d, 9 H, PMe_3, J(PH) = 13), 2.35 (m br, 2 H, C*H*PMe_3 and cage CH) 3.88 (s, 1 H, cage CH), 5.72 (d, 1 H, =CH, J(HH) = 21), 5.89 (d, 1 H, =CH, J(HH) = 21), 6.50 (d, 1 H, =CH, J(HH) = 21), 6.93 (d, 1 H, =CH, J(HH) = 21)	204.7, 197.7 (CO), 136.2, 134.6 (=*C*H$SiMe_3$), 56.1, 46.5 (cage CH), 56.1, 46.5 (cage CH), 9.8 (d, PMe_3, J(PC) = 52), 2.4 ($SiMe_3$), 0.9 (*C*H$SiMe_3$), −0.9, −1.1 ($SiMe_3$)[e]	3.3 (1 B, BCP), −1.7 (1 B, B−C), −6.1 (2 B), −8.5 (1 B, B−C), −14.0 (2 B), −22.3 (1 B), −23.8 (1 B)

[a] Units and conditions: chemical shifts (δ) in ppm; coupling constants (J) in Hz; measurements in CD_2Cl_2 as solvent; room temperature unless otherwise stated. [b] Resonances for terminal BH protons occur as broad unresolved signals in the range δ *ca.* −2 to 3. [c] Hydrogen-1 decoupled; chemical shifts are positive to high frequency of $SiMe_4$. [d] Hydrogen-1 decoupled; chemical shifts are positive to high frequency of BF_3·Et_2O (external). [e] Signal due to =*C*HB carbon nuclei not observed, probably due to broadening by ^{11}B nuclei. [f] Resonance for quaternary carbon *C*Me_3 nuclei not observed.

Downloaded by CARLI CONSORTIUM on June 30, 2009
Published on March 19, 1996 on http://pubs.acs.org | doi: 10.1021/om950934+

there is spectroscopic evidence for dissociation of THF from **3a** in CH_2Cl_2 to give the 16-electron ruthenium complex [Ru(CO)$_2$(η^5-7,8-$C_2B_9H_{11}$)].[1] Although the acetonitrile group in **3c** can be replaced by other ligands the reactions proceed less readily than those with **3a**, resulting in the latter being the reagent of choice as a synthon, as described below.

The complex [Ru(CO)$_2$(CNBu^t)(η^5-7,8-$C_2B_9H_{11}$)] (**3d**) is readily obtained by adding 1 equiv of CNBu^t to **3a**, the latter being generated from **2** and used *in situ*. The coordinated isocyanide ligand is revealed by a band in the IR spectrum at 2192 cm^{-1}, and the customary two CO absorptions for species containing a Ru(CO)$_2$(η^5-7,8-$C_2B_9H_{11}$) group are seen at 2067 and 2023 cm^{-1} (Table 1). The NMR data (Table 2) are in agreement with the formulation of **3d**. Thus, the ^{13}C{^{1}H} NMR spectrum had a broad resonance for the ligated carbon of the *C*NBu^t group at δ 134.2 and signals for the Bu^t group at δ 60.3 (*C*Me_3) and 30.5 (C*Me*$_3$). A peak for the CO groups occurred at δ 193.1, and a signal diagnostic for the cage carbon atoms was observed at δ 44.1.[2] Similar treatment of CH_2Cl_2 solutions of **3a** with PPh_3 give [Ru(CO)$_2$(PPh_3)(η^5-7,8-$C_2B_9H_{11}$)] (**3e**), characterized by the data in Tables 1 and 2. The complex is also formed from **3b** and PPh_3, but the reaction is much less facile, requiring heating in toluene. The ^{31}P{^{1}H} NMR spectrum of **3e** displayed a singlet resonance at δ 42.3.

Passage of a stream of C_2H_4 for a few minutes through a CH_2Cl_2 solution of **3a** gives [Ru(CO)$_2$(C_2H_4)(η^5-7,8-$C_2B_9H_{11}$)] (**4a**). The coordinated ethylene molecule is revealed in the ^{1}H NMR spectrum by a sharp singlet at δ 3.80 and in the ^{13}C{^{1}H} NMR spectrum by a resonance at δ 64.6. These data may be compared with those for the isolobally related cyclopentadienyl species [Fe(CO)$_2$(C_2H_4)(η^5-C_5H_5)][BF_4], which has signals in its NMR spectra for the ethylene ligand at δ 3.75 (^{1}H) and 56.86 (^{13}C{^{1}H}).[3]

The propene complex [Ru(CO)$_2$(MeCH=CH_2)(η^5-7,8-$C_2B_9H_{11}$)] (**4b**) was prepared similarly from **4a**. Because **4b** has a propylene group instead of an ethylene ligand, asymmetry is introduced. There is no longer a mirror plane through the Ru atom, the midpoints of the C=C bond, the cage C−C connectivity, and the boron atom located in the β-site with respect to the carbons in the CCB*B*B ring. This results in the appearance of two resonances for the cage CH protons (δ 2.68 and 2.86) in the ^{1}H NMR spectrum, and correspondingly in the ^{13}C{^{1}H} spectrum there are two peaks (δ 51.0 and 51.4) for the cage carbons. However, only one signal is seen for the CO ligands (δ 196.2). The ligated alkene carbons display resonances at δ 66.6 and 90.6 (Table 2).

Three signals of relative intensity 1:1:1 are observed for the CH=CH_2 group in the ^{1}H NMR spectrum of **4b**, and these occur as two doublets at δ 3.65 (J(HH) = 8 Hz) and δ 3.82 (J(HH) = 14 Hz) and a multiplet at δ 4.78. These data compare with a similar pattern of two doublets and a multiplet resonance seen for the CH=CH_2 fragments in the ^{1}H NMR spectra of [Fe(CO)$_2$(Me-CH=CH_2)(η^5-C_5H_5)][BF_4] (δ 3.43 (J(HH) = 14.7 Hz), 3.84 (J(HH) = 8.3 Hz), and 5.08 m),[3] and [Ru(CO)$_2$-(Pr^{n}CH=CH_2)(η^5-C_5H_5)][BPh_4] (δ 3.88 (J(HH) = 14 Hz), 3.90 (J(HH) = 8 Hz), and 5.25 m).[4] In all three spectra the multiplet resonance is due to the CH group and the two doublets are due to the nonequivalent hydrogens of the CH_2 group. Moreover, the doublet in each spectrum showing a ^{1}H−^{1}H coupling of *ca.* 14 Hz can be assigned to the proton of the CH_2 moiety transoid to CH, and that with a coupling of *ca.* 8 Hz to the proton cisoid to the CH group.[5]

The trimethylvinylsilane complex [Ru(CO)$_2$(Me$_3$-SiCH=CH_2)(η^5-7,8-$C_2B_9H_{11}$)] (**4c**) was also prepared and characterized by the data given in Tables 1 and 2. In the ^{1}H NMR spectrum of this complex the signals for the alkene protons appear as doublets of doublets at δ 3.44 (J(HH) = 12 and 17 Hz), 3.97 (J(HH) = 17 and 1 Hz), and 4.08 (J(HH) = 12 and 1 Hz). In the ^{13}C{^{1}H}

(2) Brew, S. A.; Stone, F. G. A. *Adv. Organomet. Chem.* **1993**, *35*, 135.
(3) Faller, J. W.; Johnson, B. V. *J. Organomet. Chem.* **1975**, *88*, 101.
(4) Gafoor, M. A.; Hutton, A. T.; Moss, J. R. *J. Organomet. Chem.*, in press.
(5) Pretsch, E.; Clerc, T.; Seibl, J.; Simon, W. *Spectral Data for Structure Determination of Organic Compounds*, 2nd ed.; Springer-Verlag: New York, 1989.

Downloaded by CARLI CONSORTIUM on June 30, 2009
Published on March 19, 1996 on http://pubs.acs.org | doi: 10.1021/om950934+

NMR spectrum resonances for the two nonequivalent alkene-ligated carbons are seen at δ 71.1 and 80.8. However, only one signal is observed for the cage carbons (δ 50.1), but this peak is very broad and can be attributed to an overlap of two resonances. The $^{13}C\{^1H\}$ NMR spectrum of **4c**, unlike that of **4b**, displays two resonances for the CO groups but with very similar chemical shifts (δ 196.3 and 196.7).

The bicyclo[2.2.1]heptene (norbornene) complex [Ru(CO)$_2$(C_7H_{10})(η^5-7,8-$C_2B_9H_{11}$)] (**4d**) was also isolated (Tables 1 and 2). Since norbornene is a symmetric alkene, in the $^{13}C\{^1H\}$ NMR spectrum of **4d** the cage carbon atoms give rise to a single peak (δ 52.6), as do the two carbons of the C=C group (δ 86.6) ligating the ruthenium. Similarly, in the ^1H NMR spectrum the protons of the cage CH groups and those of the coordinated CH=CH group appear as singlets at δ 2.58 and 4.35, respectively.

The reaction between the alkynes RC≡CR (R = Me, Ph) and **3a** yielded the alkyne complexes [Ru(CO)$_2$(RC≡CR)(η^5-7,8-$C_2B_9H_{11}$)] (R = Me (**5a**), or Ph (**5b**)). Data listed in Tables 1 and 2 fully characterize these species. In the ^1H NMR spectrum of **5a** the resonance for the Me groups of the alkyne appears as a singlet at δ 2.44, compared with a peak for these groups at δ 1.67 in the free alkyne. In the $^{13}C\{^1H\}$ NMR spectrum the coordinated carbons of **5a** resonate at δ 63.8 and the *C*H$_3$ nuclei at δ 10.2, whereas these nuclei give peaks at δ 74.6 and 3.2, respectively, in free MeC≡CMe.

It was anticipated that the but-2-yne ligand in **5a**, formally a complex of Ru^{II}, would be susceptible to nucleophilic attack. Treatment with K[BH(CHMeEt)$_3$], in OEt$_2$, followed by addition of 18-crown-6, gave the salt [K(18-crown-6)][Ru{C(Me)=C(H)Me}(CO)$_2$(η^5-7,8-$C_2B_9H_{11}$)] (**6**). As expected for a complex anion, the CO stretching bands observed for **6** (2004 and 1942 cm^{-1}) are at an appreciably lower frequency than those of **5a** (2066 and 2019 cm^{-1}). The ^1H NMR spectrum of **6** shows signals for the Me groups at δ 1.65 and 2.26, the former appearing as a partially resolved doublet of quartets (J(HH) = 7 and 1.5 Hz) and the latter a multiplet from which a $^1H-^1H$ coupling of 1.5 Hz could be measured. The vinyl group proton C(Me)=C(*H*)Me is seen as a partially resolved quartet of quartets at δ 5.95 (J(HH) = 7 and 1.5 Hz). This pattern is virtually identical with that observed in the spectrum of *trans*-MeC(H)=C(Me)I,[6] and accordingly we assign a *trans* configuration for the Me groups in **6**. The $^{13}C\{^1H\}$ NMR spectral pattern for the RuC(Me)=C(H)Me group of **6** is also similar to that of *trans*-MeC(H)=C(Me)I. The spectrum of the former has resonances for the Me substituents at δ 20.4 and 38.8 and for the C=C nuclei at δ 126.2 and 143.9. In the $^{13}C\{^1H\}$ NMR spectrum of *trans*-MeC(H)=C(Me)I the corresponding peaks occur at δ 22.4 and 33.4 (Me), and 102.4 and 130.0 (C=C).

The reaction between PPh$_3$ and **5a** was next investigated to establish whether the MeC≡CMe ligand would be displaced by the phosphine, yielding **3e**, or whether the coordinated alkyne would be attacked by the phosphine to give an ylide complex. It was evident from microanalytical and spectroscopic data that the product of the reaction was [Ru{C(Me)=C(Me)PPh$_3$}(CO)$_2$(η^5-7,8-$C_2B_9H_{11}$)] (**7**). The $^{31}P\{^1H\}$ NMR spectrum showed a singlet resonance at δ 9.92, the chemical shift being very different from that displayed by **3e** (δ 42.3). In the ^1H NMR spectrum the resonances for the Me groups of the C(Me)=C(Me)PPh$_3$ moiety were seen as two multiplets centered at δ 2.10 and δ 2.46, each of an intensity corresponding to three protons. The former consisted of two sets of peaks separated by 15 Hz. Evidently $^{31}P-^1H$ coupling arises through proximity of the PPh$_3$ group. The $^{13}C\{^1H\}$ NMR spectrum showed peaks for the *C*Me nuclei of the C(Me)=C(Me) unit at δ 122.4 (J(PC) = 82 Hz) and 107.5 (J(PC) = 51 Hz) and for the C*Me* nuclei at δ 43.3 (J(PC) = 19 Hz) and 29.1 (J(PC) = 24 Hz).

Reactions between **3a** and the alkynes RC≡CH (R = Bu^t, SiMe$_3$) were next studied. Several products were formed, the proportions of which critically depended on the stoichiometry employed. Reactions involving the reactants in a 1:1 mole ratio will be discussed first and those in which a large excess of the alkyne was used later. When 1 equiv of Bu^{t}C≡CH was added to **3a** in CH_2Cl_2, the complex [Ru(CO)$_2$(η^2:η^5-C(H)=C(H)Bu^t-7,8-$C_2B_9H_{10}$)] (**8**) was by far the major product. Examination of the NMR spectra of **8**, discussed in detail below, revealed that it was formed as a mixture of the two isomers **8a** and **8b**, in which the former predominated to a slight degree. Also visible in the ^1H and $^{11}B\{^1H\}$ NMR spectra were some low-intensity peaks indicating the presence of very small amounts of the product formed when, as discussed later, an excess of the alkyne is used.

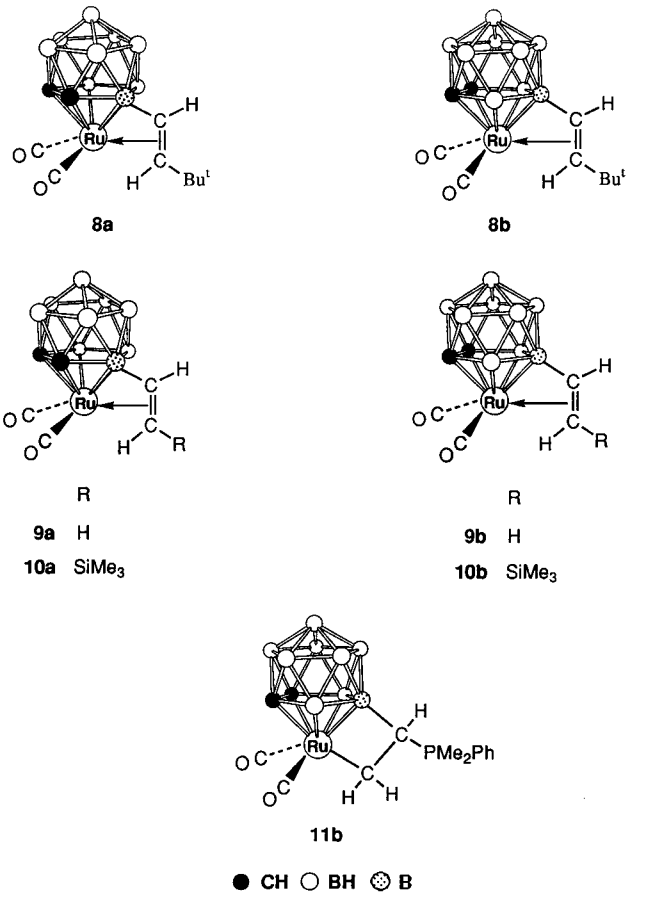

The isomers **8a** and **8b** differ in the site of attachment of the C(H)=C(H)Bu^t substituent to the boron atoms in the open CCBBB pentagonal face of the *nido*-C_2B_9 cage coordinated to the ruthenium. Although these isomers

(6) Garner, C. M; Prince, M. E. Unpublished results.

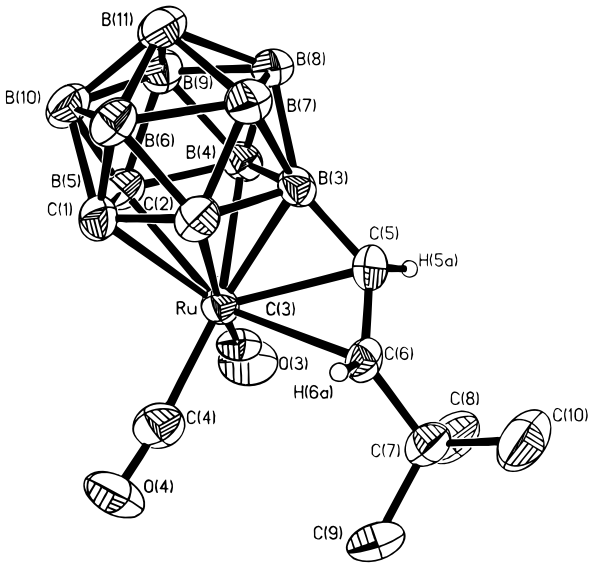

Figure 1. Structure of $[Ru(CO)_2(\eta^2{:}\eta^5\text{-}9\text{-}C(H){=}C(H)Bu^t\text{-}7,8\text{-}C_2B_9H_{10})]$ (**8a**), showing the crystallographic labeling scheme. Except for H(5a) and H(6a), hydrogen atoms are omitted for clarity and thermal ellipsoids are shown at the 50% probability level.

were not separable by column chromatography, it was possible to grow crystals from solutions of mixtures and carry out an X-ray diffraction study. The crystals thus obtained were those of the predominant isomer $[Ru(CO)_2(\eta^2{:}\eta^5\text{-}9\text{-}C(H){=}C(H)Bu^t\text{-}7,8\text{-}C_2B_9H_{10})]$ (**8a**), in which the exopolyhedral C(H)═C(H)Bu^t group on the icosahedral 3,1,2-RuC_2B_9 framework is bonded to a boron α to the carbon atoms in the CCB*B*B ring.

The molecular structure is shown in Figure 1, and selected internuclear distances and angles for **8a** are listed in Table 3. The ruthenium atom is η^5-coordinated by the open face of the *nido*-C_2B_9 cage but in addition is also η^2-coordinated by the C═C bond of the pendant C(H)═C(H)Bu^t group. The transoid hydrogen atoms H(5a) and H(6a) were located by electron density mapping. Two terminally bound CO groups are attached to the metal atom, in agreement with the observation of two carbonyl stretches in the IR spectrum (Table 1). Thus, the various groups attached to the ruthenium provide the necessary number of electrons for a filled valence shell.

It is likely that in the reaction between **3a** and Bu^{t}C≡CH the alkyne molecule of the initially formed complex $[Ru(CO)_2(Bu^tC{\equiv}CH)(\eta^5\text{-}7,8\text{-}C_2B_9H_{11})]$ inserts into a B−H bond in the CCBBBB face of the cage, giving one or the other of the isomers **8**. There is precedent for such a process. Protonation of $[NEt_4][Mo(CO)_2(\eta^3\text{-}C_3H_5)(\eta^5\text{-}7,8\text{-}C_2B_9H_9)]$ with $HBF_4{\cdot}Et_2O$ in the presence of $Me_3SiC{\equiv}CSiMe_3$ yields a mixture of the two complexes $[Mo(CO)(Me_3SiC{\equiv}CSiMe_3)_2(\eta^5\text{-}7,8\text{-}C_2B_9H_{11})]$ and $[Mo(CO)_3(\eta^2{:}\eta^5\text{-}10\text{-}C(H){=}C(H)SiMe_3\text{-}7,8\text{-}C_2B_9H_{10})]$, formed in almost equal amounts.[7] The latter is structurally akin to the complexes **8** but has a cage with a C(H)═C(H)SiMe$_3$ substituent. It evidently forms as a result of C−SiMe$_3$ bond cleavage of $Me_3SiC{\equiv}CSiMe_3$ at some stage during the reaction. Along the reaction pathway the vinylidene group Mo═C═C(H)SiMe$_3$ is probably present, which subsequently inserts into a cage B−H bond to give the species $[Mo(CO)_3(\eta^2{:}\eta^5\text{-}10\text{-}C(H){=}C(H)SiMe_3\text{-}7,8\text{-}C_2B_9H_{10})]$.[7] It seems likely that formation of the isomers **8** also involves a species containing a vinylidene group, Ru═C═C(H)Bu^t, in which case it would insert into an adjacent B−H bond on the icosahedral 3,1,2-RuC_2B_9 framework.[2] Rearrangement of metal-coordinated η^2-RC≡CH groups into vinylidene moieties is well-established and has been the subject of much study and conjecture as to the mechanism.[8−12]

Although the structures of **8a** and $[Mo(CO)_3(\eta^2{:}\eta^5\text{-}10\text{-}C(H){=}C(H)SiMe_3\text{-}7,8\text{-}C_2B_9H_{10})]$ differ in the position of attachment of the vinyl groups to their respective CCBBB rings (B(9) versus B(10) sites, respectively), there are similarities. Thus, the hydrogen atoms in the C(H)═C(H) groups are transoid in both complexes, and the C═C distances (1.398(7) Å for **8a** and 1.42(2) Å for the molybdenum complex) are comparable, as are the B−C(H) bond lengths (1.531(8) Å for **8a** and 1.53(2) Å for the molybdenum complex).

The isomers **8a** and **8b** could not be separated by column chromatography. Nevertheless, since they were formed in a *ca.* 60:40 ratio, peaks for the individual isomers in the NMR spectra of mixtures were readily assigned (Table 2) on the basis of their relative intensities. Both isomers are asymmetric; hence, in the ^{1}H NMR spectrum each isomer shows two peaks for the cage CH groups. However, the peak separations are appreciably different, being 2.32 ppm for one isomer and 0.55 ppm for the other. We infer that the pair of signals (δ 1.84 and 4.16) with the larger separation are those of **8a**, and those (δ 3.39 and 3.94) with the smaller separation are due to **8b**. This is to be expected because in **8a** the C(H)═C(H)Bu^t substituent is attached to a boron atom adjacent to a carbon in the CCBBB ring, as revealed by the X-ray analysis, whereas in **8b** the substituent is separated from both carbons by a boron atom. Hence, in **8a** the closer proximity of the C(H)═C(H)Bu^t substituent to one cage CH group would likely accentuate the chemical shift difference observed between the two CH resonances in the ^{1}H NMR spectrum. The presence of the protons in the C(H)═C(H) groups of the isomers **8** was clearly indicated from the ^{1}H NMR data. For each isomer two doublet resonances are seen for these hydrogens, at δ 4.76 and 4.86 (J(HH) = 14 Hz) for **8a** and at δ 4.90 and 5.08 (J(HH) = 13 Hz) for **8b**.

In the $^{13}C\{^1H\}$ NMR spectrum of the isomeric mixture resonances are seen at δ 57.7 and 37.4. The latter signal was very broad with an apparent intensity *ca.* 3 times that of the former. We propose that the resonance at δ 57.7 is due to one of the cage CH groups of **8a** and that the signal at δ 37.4 is due to the other CH fragment of **8a** as well as those of the more symmetrical isomer **8b**. In agreement with their nonequivalence the CO ligands of both isomers show two resonances for these groups. Peaks for the ═*C*HBu^t nuclei are seen at δ 110.0 (**8a**) and 107.5 (**8b**). The resonances for the ═*C*HB carbons of the isomers evidently overlap in a broad band at δ

(7) Dossett, S. J.; Li, S.; Mullica, D. F.; Sappenfield, E. L.; Stone, F. G. A. *J. Chem. Soc., Dalton Trans.* **1993**, 3551.

(8) Werner, H. *Angew. Chem., Int. Ed., Engl.* **1990**, *29*, 1077.
(9) Bruce, M. I. *Chem. Rev.* **1991**, *91*, 197.
(10) Silvestre, J.; Hoffmann, R. *Helv. Chim. Acta* **1985**, *68*, 1461.
(11) Wakatsuki, Y.; Yamazaki, H. *J. Organomet. Chem.* **1995**, *100*, 349.
(12) Nombel, P.; Lugan, N.; Mathieu, R. *J. Organomet. Chem.* **1995**, *503*, C22.

Downloaded by CARLI CONSORTIUM on June 30, 2009
Published on March 19, 1996 on http://pubs.acs.org | doi: 10.1021/om950934+

Table 3. Selected Internuclear Distances (Å) an Angles (deg) for [Ru(CO)$_2$(η^2:η^5-9-CH=C(H)Bu^t-7,8-C$_2$B$_9$H$_{10}$)] (8a), with Estimated Standard Deviations in Parentheses

Ru−C(1)	2.279(6)	Ru−C(2)	2.216(6)	Ru−B(3)	2.152(6)	Ru−B(4)	2.285(6)
Ru−B(5)	2.295(7)	Ru−C(3)	1.856(6)	Ru−C(4)	1.930(6)	Ru−C(5)	2.249(6)
Ru−C(6)	2.401(5)	C(1)−C(2)	1.592(8)	C(1)−B(5)	1.72(1)	C(1)−B(6)	1.73(1)
C(1)−B(10)	1.677(8)	C(2)−B(3)	1.764(9)	C(2)−B(6)	1.686(8)	C(2)−B(7)	1.695(9)
B(3)−B(4)	1.823(9)	B(3)−B(7)	1.79(1)	B(3)−B(8)	1.773(8)	B(3)−C(5)	1.531(8)
B(4)−B(5)	1.79(1)	B(4)−B(8)	1.79(1)	B(4)−B(9)	1.770(9)	B(5)−B(9)	1.81(1)
B(5)−B(10)	1.81(1)	B(6)−B(7)	1.77(1)	B(6)−B(10)	1.76(1)	B(6)−B(11)	1.75(1)
B(7)−B(8)	1.81(1)	B(7)−B(11)	1.767(9)	B(8)−B(9)	1.80(1)	B(8)−B(11)	1.77(1)
B(9)−B(10)	1.76(1)	B(9)−B(11)	1.76(1)	B(10)−B(11)	1.76(1)	C(3)−O(3)	1.154(8)
C(4)−O(4)	1.140(8)	C(5)−C(6)	1.398(7)	C(5)−H(5a)	0.98	C(6)−C(7)	1.509(7)
C(6)−H(6a)	1.04	C(7)−C(8)	1.53(1)	C(7)−C(9)	1.53(1)	C(7)−C(10)	1.52(1)
C(1)−Ru−C(2)	41.5(2)	C(1)−Ru−B(3)	76.7(2)	C(1)−Ru−B(4)	75.9(2)	C(1)−Ru−B(5)	44.0(2)
C(1)−Ru−C(3)	134.2(2)	C(1)−Ru−C(4)	93.1(2)	C(1)−Ru−C(5)	114.4(2)	C(1)−Ru−C(6)	121.5(2)
C(2)−Ru−B(3)	47.6(2)	C(2)−Ru−B(4)	78.6(2)	C(2)−Ru−B(5)	75.3(2)	C(2)−Ru−C(3)	167.0(2)
C(2)−Ru−C(4)	103.7(2)	C(2)−Ru−C(5)	75.8(2)	C(2)−Ru−C(6)	81.3(2)	B(3)−Ru−B(4)	48.4(2)
B(3)−Ru−B(5)	80.2(2)	B(3)−Ru−C(3)	123.0(3)	B(3)−Ru−C(4)	145.0(2)	B(3)−Ru−C(5)	40.7(2)
B(3)−Ru−C(6)	68.7(2)	B(4)−Ru−C(3)	88.4(2)	B(4)−Ru−B(5)	46.1(3)	B(4)−Ru−C(4)	160.7(2)
B(4)−Ru−C(5)	74.6(2)	B(4)−Ru−C(6)	109.4(2)	B(5)−Ru−C(3)	95.1(3)	B(5)−Ru−C(4)	115.4(3)
B(5)−Ru−C(5)	117.6(2)	B(5)−Ru−C(6)	148.7(2)	C(3)−Ru−C(4)	88.1(3)	C(3)−Ru−C(5)	101.9(2)
C(3)−Ru−C(6)	104.3(2)	C(4)−Ru−C(5)	124.6(2)	C(4)−Ru−C(6)	89.8(2)	C(5)−Ru−C(6)	34.8(2)
Ru−B(3)−C(5)	73.1(3)	C(2)−B(3)−C(5)	112.6(4)	B(4)−B(3)−C(5)	109.8(5)	Ru−C(3)−O(3)	176.1(5)
Ru−C(4)−O(4)	174.7(5)	Ru−C(5)−B(3)	66.3(3)	Ru−C(5)−H(5a)	111.8(1)	B(3)−C(5)−H(5a)	121.9(3)
Ru−C(5)−C(6)	78.6(3)	B(3)−C(5)−C(6)	123.3(5)	H(5a)−C(5)−C(6)	111.8(3)	Ru−C(6)−C(5)	66.6(3)
Ru−C(6)−H(6a)	100.7(1)	C(5)−C(6)−H(6a)	121.1(3)	Ru−C(6)−C(7)	128.3(4)	C(5)−C(6)−C(7)	124.5(5)
H(6a)−C(6)−C(7)	108.6(3)	C(6)−C(7)−C(8)	113.6(5)	C(6)−C(7)−C(9)	109.5(5)	C(6)−C(7)−C(10)	105.4(5)

Downloaded by CARLI CONSORTIUM on June 30, 2009
Published on March 19, 1996 on http://pubs.acs.org | doi: 10.1021/om950934+

86.5. In the ^{11}B{^{1}H} NMR spectrum diagnostic signals are observed for the *B*C(H)=C(H)Bu^t nuclei at δ 8.1 (**8a**) and 17.8 (**8b**).[2] In fully coupled ^{11}B NMR spectra these signals remained as singlets, whereas the other resonances became doublets as a result of ^{1}H−^{11}B coupling of *ca*. 130−140 Hz.

In view of the results obtained with Bu^{t}C≡CH, it was anticipated that the reaction between Me$_3$SiC≡CH and **3a**, using a mole ratio of approximately 1:1, would yield a mixture of two isomers which differ as to the site of attachment of the C(H)=C(H)SiMe$_3$ substituent in the CCBBB pentagonal ring. However, the reaction was more complicated. Initial studies revealed that the major product formed was a mixture of isomers of the compound [Ru(CO)$_2$(η^2:η^5-CH=CH$_2$-7,8-C$_2$B$_9$H$_{10}$)] (**9**), and only very small amounts of the isomers of [Ru(CO)$_2$-(η^2:η^5-C(H)=C(H)SiMe$_3$-7,8-C$_2$B$_9$H$_{10}$)] (**10**) were formed. The presence of only traces of the latter in the mixture, as well as an ability to separate **9** into the two isomers [Ru(CO)$_2$(η^2:η^5-9-CH=CH$_2$-7,8-C$_2$B$_9$H$_{10}$)] (**9a**) and [Ru-(CO)$_2$(η^2:η^5-10-CH=CH$_2$-7,8-C$_2$B$_9$H$_{10}$)] (**9b**) by column chromatography, proved useful, greatly assisting peak assignments in the NMR spectra of the various species, as discussed below.

Complexes **9a** and **9b** evidently result from facile cleavage of C−SiMe$_3$ bonds. Similar behavior has been observed previously with Me$_3$SiC≡CH.[7] Protonation of [NEt$_4$][Mo(CO)$_2$(η^3-C$_3$H$_5$)(η^5-7,8-C$_2$B$_9$H$_{11}$)] in the presence of the alkyne gives a mixture of [Mo(CO)$_3$(η^2:η^5-10-C(H)=C(H)SiMe$_3$-7,8-C$_2$B$_9$H$_{10}$)] and [Mo(CO)-(HC≡CH)$_2$(η^5-7,8-C$_2$B$_9$H$_{11}$)], the ethyne species having formed by generation of HC≡CH from Me$_3$SiC≡CH. Interestingly, we found that a mixture of the isomers **9** could be obtained directly from **3a** by adding calcium carbide and water to CH$_2$Cl$_2$ solutions of the THF complex, thus generating ethyne *in situ*.

From experiments described below it became evident that the presence of small amounts of water caused loss of SiMe$_3$ groups, leading to **9a** and **9b**. Water might inadvertently be introduced into the reaction via the glassware or in trace amounts via the solvents, even though the latter were vigorously dried. Conversion of Me$_3$SiC≡CH into HC≡CH through dismutation is improbable, since the isomers **9** were not formed even in trace amounts in the reaction between **3a** and Bu^{t}C≡CH. Moreover, the species **9** were not formed from **10**, because treatment of mixtures of **9** and **10** with water decomposed the former while the latter remained unreacted.

In the various syntheses described herein, the reagent **3a** was prepared *in situ* from **2** and used without prior isolation. This procedure was followed because prior isolation of **3a** as a solid, followed by subsequent preparation of solutions in CH$_2$Cl$_2$, appreciably diminished the yield of desired end product. However, if **3a** is prepared and used *in situ*, the likelihood of water contamination is increased since more steps in the method are required. To test this possibility, a solid sample of compound **3a** was isolated, purified,[1] and dissolved in CH$_2$Cl$_2$. This solution was then treated with Me$_3$SiC≡CH. Examination of the ^{1}H NMR spectra of the mixture, prior to chromatography, revealed that although both compounds **9** and **10** had formed, significantly, the proportion of the latter was very greatly enhanced to *ca*. 60% of total product, as estimated from relative peak intensities in the NMR spectra. This compares with a maximum of *ca*. 10% of **10** produced when **3a** is prepared *in situ* and treated with Me$_3$-SiC≡CH. In a further experiment a sample of **3a** was isolated as a solid, dissolved in CH$_2$Cl$_2$, and treated with Me$_3$SiC≡CH to which a drop of water had been added. Examination of the mixture after completion of the reaction revealed formation of the isomers **9** with only trace amounts of the species **10** being present.

Trimethylsilyl groups are very susceptible to cleavage, and the η^2-alkyne complex [Ru(CO)$_2$(Me$_3$SiC≡CH)(η^5-7,8-C$_2$B$_9$H$_9$)] could provide a pathway for C−Si bond fission. Although it was not isolated in the present work, it is reasonable to propose that such an η^2-alkyne species would be an intermediate from **3a** to **10**. Moreover, it is likely that this intermediate would to be very susceptible to nucleophilic attack, as was

Table 4. Selected Internuclear Distances (Å) and Angles (deg) for [Ru(CO)$_2$(σ,η^5-10-C(H)(PMe$_2$Ph)CH$_2$-7,8-C$_2$B$_9$H$_{10}$)] (11b), with Estimated Standard Deviations in Parentheses

Ru(1)−C(1)	2.33(1)	Ru(1)−C(2)	2.31(1)	Ru(1)−B(3)	2.23(1)	Ru(1)−B(4)	2.237(8)
Ru(1)−B(5)	2.32(1)	Ru(1)−C(4)	2.142(9)	Ru(1)−C(11)	1.80(1)	Ru(1)−C(12)	1.84(1)
C(11)−O(11)	1.17(2)	C(12)−O(12)	1.17(2)	C(1)−C(2)	1.61(2)	C(1)−B(5)	1.780(1)
C(1)−B(6)	1.69(2)	C(1)−B(10)	1.74(2)	C(2)−B(3)	1.61(1)	C(2)−B(6)	1.67(2)
C(2)−B(7)	1.72(2)	B(3)−B(4)	1.73(1)	B(3)−B(7)	1.79(2)	B(3)−B(8)	1.74(1)
B(4)−B(5)	1.81(2)	B(4)−B(8)	1.80(2)	B(4)−B(9)	1.81(2)	B(4)−C(3)	1.61(1)
B(5)−B(9)	1.77(2)	B(5)−B(10)	1.73(2)	B(6)−B(7)	1.78(2)	B(6)−B(10)	1.79(2)
B(6)−B(11)	1.84(1)	B(7)−B(8)	1.79(1)	B(7)−B(11)	1.79(2)	B(8)−B(9)	1.77(2)
B(8)−B(11)	1.74(2)	B(9)−B(10)	1.73(1)	B(9)−B(11)	1.74(2)	B(10)−B(11)	1.80(2)
C(3)−H(3a)	0.96	C(3)−C(4)	1.50(1)	C(3)−P(1)	1.786(9)	C(4)−H(4a)	0.95
C(4)−H(4b)	0.98	P(1)−C(5)	1.77(1)	P(1)−C(6)	1.77(1)	P(1)−C(21)	1.787(9)
C(21)−C(22)	1.42(1)	C(21)−C(26)	1.37(1)	C(22)−C(23)	1.38(2)	C(23)−C(24)	1.34(2)
C(24)−C(25)	1.37(2)	C(25)−C(26)	1.41(2)				

C(1)−Ru(1)−C(2)	40.6(4)	C(1)−Ru(1)−B(3)	72.1(4)	C(1)−Ru(1)−B(4)	76.7(3)	C(1)−Ru(1)−B(5)	45.0(3)
C(1)−Ru(1)−C(4)	136.7(3)	C(2)−Ru(1)−B(3)	41.7(3)	C(2)−Ru(1)−B(4)	74.2(3)	C(2)−Ru(1)−B(5)	73.0(4)
C(2)−Ru(1)−C(4)	135.0(3)	B(3)−Ru(1)−B(4)	45.5(3)	B(3)−Ru(1)−B(5)	76.0(4)	B(3)−Ru(1)−C(4)	93.9(4)
B(4)−Ru(1)−B(5)	46.8(4)	B(4)−Ru(1)−C(4)	65.4(4)	B(5)−Ru(1)−C(4)	92.2(4)	C(11)−Ru(1)−C(2)	130.0(4)
C(11)−Ru(1)−C(12)	89.8(5)	C(11)−Ru(1)−C(1)	97.4(5)	C(11)−Ru(1)−B(3)	169.4(5)	C(11)−Ru(1)−B(4)	131.9(4)
C(11)−Ru(1)−B(5)	95.7(5)	C(11)−Ru(1)−C(4)	92.9(4)	C(12)−Ru(1)−C(1)	132.4(4)	C(12)−Ru(1)−C(2)	102.0(5)
C(12)−Ru(1)−B(3)	98.3(5)	C(12)−Ru(1)−B(4)	129.5(5)	C(12)−Ru(1)−B(5)	174.2(5)	C(12)−Ru(1)−C(4)	89.3(5)
Ru(1)−B(4)−C(3)	94.0(5)	B(3)−B(4)−C(3)	126.3(8)	B(5)−B(4)−C(3)	114.7(8)	B(8)−B(4)−C(3)	133.4(7)
B(9)−B(4)−C(3)	127.3(6)	B(4)−C(3)−H(3a)	109.2(5)	B(4)−C(3)−C(4)	98.9(6)	H(3a)−C(3)−C(4)	105.7(6)
B(4)−C(3)−P(1)	119.1(7)	H(3a)−C(3)−P(1)	108.4(3)	C(4)−C(3)−P(1)	114.5(7)	Ru(1)−C(4)−C(3)	101.2(6)
Ru(1)−C(4)−H(4a)	110.8(3)	C(3)−C(4)−H(4a)	113.4(6)	Ru(1)−C(4)−H(4b)	109.9(3)	C(3)−C(4)−H(4b)	110.9(6)
Ru(1)−C(11)−O(11)	176.8(11)	Ru(1)−C(12)−O(12)	179.3(7)	C(3)−P(1)−C(5)	111.8(4)	C(3)−P(1)−C(6)	110.7(5)
C(3)−P(1)−C(21)	106.9(4)	C(5)−P(1)−C(6)	109.3(5)	C(5)−P(1)−C(21)	108.7(5)	C(6)−P(1)−C(21)	109.4(4)

Downloaded by CARLI CONSORTIUM on June 30, 2009
Published on March 19, 1996 on http://pubs.acs.org | doi: 10.1021/om950934+

demonstrated for the structurally related complex **5a**. Water molecules might induce loss of Me_3SiOH from a $Me_3SiC{\equiv}CH$ molecule ligated to Ru^{II}, thereby producing a HC≡CH complex. The ^{1}H NMR spectra of all the mixtures obtained in the reactions revealed no resonance for $Me_3SiC{\equiv}CSiMe_3$ but a strong signal was observed at δ 0.065 which correlates with that reported for $Me_3SiOSiMe_3$,[13] the product expected by water cleavage of $SiMe_3$ groups. However, at present there is insufficient knowledge available as to precisely at what stage in the reactions cleavage of the $SiMe_3$ groups occurs.

Isomers **9a** and **9b** are produced in an approximate 1:4 ratio, and as mentioned above they can be separated. The ^{1}H NMR spectra (Table 2) of both species show resonances for the nonequivalent cage CH groups. These occur at δ 1.72 and 4.20 for **9a** and at δ 3.52 and 3.98 for **9b**. The chemical shift difference between the CH signals is larger for **9a**, as expected, since it is the isomer with the CH=CH$_2$ substituent attached to the boron atom in the α-site in the CC*B*BB ring coordinated to the metal. The CH=CH$_2$ groups in both isomers show a pattern of three peaks. The resonance for the =C*H*B proton occurs as a doublet of doublets [**9a**, δ 4.96, with J(HH) = 10 and 14 Hz; **9b**, δ 5.01, with J(HH) = 10 and 13 Hz), due to cisoid and transoid coupling with the protons of the =CH$_2$ group. The =CH$_2$ moiety in **9a** gives rise to two doublet signals at δ 3.36 (J(HH) = 14 Hz) and 4.35 (J(HH) = 10 Hz). The peak at δ 3.36 has the larger ^{1}H−^{1}H coupling and must be due to the proton in the =CH$_2$ group transoid to =C*H*B.[5] For **9b** the resonances for the =CH$_2$ protons are less well resolved, occurring as a doublet at δ 3.72 (J(HH) = 13 Hz) and a broad peak at δ 4.41.

In the ^{13}C{^{1}H} NMR spectra only one resonance is observed for the cage CH groups of **9b** (δ 38.6), whereas in the spectrum of **9a** two signals for these groups are observed (δ 59.0 and 38.6). No signal was seen in the ^{13}C{^{1}H} NMR spectrum of either isomer for the *C*(H)B nuclei, but this is not unusual for exopolyhedral cage carbons. Absence of the resonance is attributable to quadrupolar broadening by adjacent ^{11}B nuclei.[2] The ^{11}B{^{1}H} NMR spectrum of each isomer shows nine distinct resonances, in agreement with the asymmetry in each molecule. A peak seen at δ 9.4 for **9a** and one at δ 18.9 for **9b**, with the observation that these signals remain singlets in fully coupled ^{11}B NMR spectra, is in agreement with their being due to the BC(H) nuclei.[2] No interconversion between the two isomers was observed when a sample of **9b** was heated in toluene for 24 h.

The NMR data (Table 2) for the isomers of **10** were also in agreement with their formulations. Assignments are from measurements made on mixtures in which **10b** was the major component, relative peak intensities being used to identify bands. As expected, the disparity of chemical shifts between the cage CH resonances is substantially smaller for **10b** than for **10a**, since in the former the cage C(H)=C(H)SiMe$_3$ substituent is attached to a boron further from the carbons in the CCB*B*B ring. In the ^{11}B{^{1}H} NMR spectra peaks for the boron nuclei of the BC(H) groups are observed for **10a** at δ 10.2 and for **10b** at δ 20.0. These signals remained as singlets in the ^{11}B NMR spectrum.

A heptane solution of **9**, having isomer **9b** as the major component, was treated with PMe$_2$Ph to determine if the phosphine would ligate the ruthenium atom by displacing the η^2 interaction of the C(H)=CH$_2$ group with the metal, or whether the phosphine would attack a carbon atom of the pendant vinyl group. Both NMR measurements and an X-ray diffraction study established that the latter process occurred, the product being [Ru(CO)$_2$(σ,η^5-10-C(H)(PMe$_2$Ph)CH$_2$-7,8-C$_2$B$_9$H$_{10}$)] (**11b**).

Selected parameters from an X-ray diffraction study are listed in Table 4 and the molecule is shown in Figure 2. It is immediately apparent that the complex **11b** is zwitterionic, necessitating a formal positive charge on the phosphorus atom attached to C(3) and a negative

(13) Aldrich Library of ^{13}C and ^{1}H FT NMR Spectra, *FT-NMR* **1** (3), 672B.

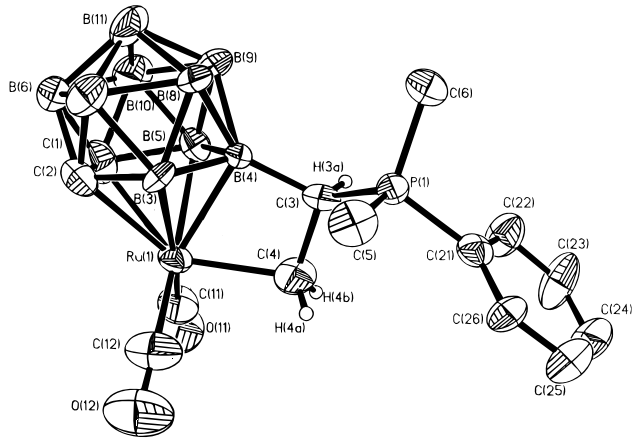

Figure 2. Structure of $[Ru(CO)_2(\sigma,\eta^5\text{-}10\text{-}C(H)(PMe_2Ph)\text{-}CH_2\text{-}7,8\text{-}C_2B_9H_{10})]$ (**11b**), showing the crystallographic labeling scheme. Except for H(3a), H(4a), and H(4b), hydrogen atoms are omitted for clarity and thermal ellipsoids are shown at the 50% probability level.

charge associated with the RuC_2B_9 framework. As anticipated, since **9b** was the dominant isomer in the precursor, the exo-polyhedral $C(H)(PMe_2Ph)CH_2$ group is linked to B(4), the boron atom in the β-site with respect to the two carbons in the CCB*B*B face of the cage. The B(4)−C(3) distance (1.61(1) Å) is perceptibly longer than B(3)−C(5) (1.531(8) Å) in **8a**, reflecting the different hybridizations of the carbon atoms in the two molecules. The ruthenium atom is attached to the CH_2 group (Ru−C(4) = 2.142(9) Å] of the $C(H)(PMe_2Ph)CH_2$ moiety and is η^5-coordinated by the *nido*-C_2B_9 cage framework in the usual manner. The two terminal CO ligands complete the coordination at the metal center. The CO stretching bands at 1998 and 1934 cm^{-1} are at appreciably lower frequency than those of the precursor **9b** (2054 and 2005 cm^{-1}), as expected, because of the negative charge associated with the RuC_2B_9 group in **11b**.

The NMR data (Table 2) are in agreement with the results of the X-ray diffraction study. The $^{31}P\{^1H\}$ NMR spectrum of **11b** showed a strong singlet resonance at δ 20.1, but there was a much weaker resonance at δ 19.8, which we ascribe to its isomer $[Ru(CO)_2(\sigma,\eta^5\text{-}9\text{-}C(H)(PMe_2Ph)CH_2\text{-}7,8\text{-}C_2B_9H_{10})]$ (**11a**). The latter is likely to form in small amounts, since the precursor **9** contained both **9a** and **9b** in a ratio of *ca.* 1:4. There were nine signals in the $^{11}B\{^1H\}$ NMR spectrum. A resonance at δ −6.4 can be assigned to the *B*C(H)(PMe_2-Ph) nucleus of **11b** because it remains as a singlet in a fully coupled ^{11}B spectrum, whereas the other peaks become doublets through $^1H-^{11}B$ coupling. The ^1H NMR spectrum displays the expected signals for **11b**; however, some peaks were duplicated by weak signals attributable to the presence of a small amount of **11a**. The $^{13}C\{^1H\}$ spectrum shows two resonances for the CO ligands (δ 199.7 and 197.7) and two peaks for the cage CH groups (δ 44.5 and 38.8). A doublet signal at δ 123.2 with a $^{31}P-^{13}C$ coupling of 36 Hz is probably due to the C^1 nucleus of the Ph group rather than to the B*C*(H)-PMe_2Ph nucleus. The signal for the latter would be broad and also have $^{31}P-^{13}C$ coupling and, evidently, was too weak to be seen.

As mentioned earlier, while the reaction between the alkyne $Bu^tC{\equiv}CH$ and **3a** in 1:1 mole ratio gave the isomers **8** as the main product, trace amounts of another species were detected by NMR spectroscopy. A similar observation was made with $Me_3SiC{\equiv}CH$ as reactant. The nature of these minor species $[Ru(CO)_2\{\eta^2{:}\eta^5\text{-}9\text{-}C(H){=}C(H)Bu^t\text{-}10,11\text{-}[C(H){=}C(H)Bu^t]_2\text{-}7,8\text{-}C_2B_9H_8\}]$ (**12a**) and $[Ru(CO)_2\{\eta^2{:}\eta^5\text{-}9\text{-}C(H){=}C(H)SiMe_3\text{-}10,11\text{-}[C(H){=}C(H)SiMe_3]_2\text{-}7,8\text{-}C_2B_9H_8\}]$ (**12b**) became evident when they were formed in good yield as essentially the only products when **3a** and **3c** were treated with a large excess of the alkynes RC≡CH.

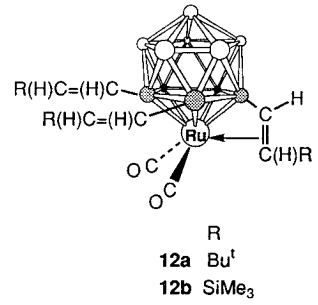

R
12a Bu^t
12b $SiMe_3$

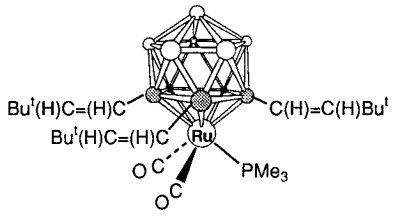

13

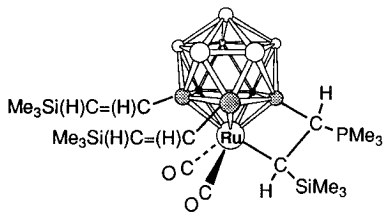

14

● CH ○ BH ◍ B

Data obtained for the complexes **12** (Tables 1 and 2) made it apparent that reaction had occurred with insertion of alkyne molecules into all three B−H bonds present in the CCBBB rings ligating the ruthenium atoms. Moreover, one of the C(H)=C(H)R substituents in **12a** and **12b** was η^2-coordinated to the ruthenium center. The NMR spectra were very informative. In the $^{11}B\{^1H\}$ NMR spectrum (Table 2) of **12b** there were nine distinct signals. In a fully coupled ^{11}B spectrum six of these peaks became doublets due to $^1H-^{11}B$ coupling, while three at δ 17.5, 10.3, and −2.0 remained as singlets and thus may be assigned to boron atoms bonded to exo-polyhedral carbons. The $^{11}B\{^1H\}$ NMR spectrum of **12a** displayed eight bands, but one was of an intensity indicating an overlap of two signals. Again, in a fully coupled ^{11}B NMR spectrum three resonances (δ 15.4, 10.9, and −2.5) showed no $^1H-^{11}B$ coupling.

The ^1H NMR spectra of both **12a** and **12b** showed six resonances for the protons of the C(H)=C(H)R groups, as expected for three different environments of these substituents. The observed $^1H-^1H$ couplings (12−21 Hz) of the vinylic protons do not allow a distinction between cisoid and transoid arrangements for the

Downloaded by CARLI CONSORTIUM on June 30, 2009
Published on March 19, 1996 on http://pubs.acs.org | doi: 10.1021/om950934+

Table 5. Selected Internuclear Distances (Å) and Angles (deg) for [Ru(CO)$_2$(PMe$_3$){η^5-9,10,11-[C(H)=C(H)Bu^t]$_3$-7,8-C$_2$B$_9$H$_8$}] (13), with Estimated Standard Deviations in Parentheses

Ru(1)−C(1)	2.219(6)	Ru(1)−C(2)	2.226(6)	Ru(1)−B(3)	2.321(7)	Ru(1)−B(4)	2.378(8)
Ru(1)−B(5)	2.270(8)	Ru(1)−C(3)	1.896(9)	Ru(1)−C(4)	1.874(9)	Ru(1)−P(1)	2.359(2)
C(1)−C(2)	1.631(9)	C(1)−B(5)	1.75(1)	C(1)−B(6)	1.74(1)	C(1)−B(10)	1.710(10)
C(2)−B(3)	1.727(9)	C(2)−B(6)	1.72(1)	C(2)−B(7)	1.68(1)	B(3)−B(4)	1.901(10)
B(3)−B(7)	1.79(1)	B(3)−B(8)	1.79(1)	B(3)−C(11)	1.59(1)	B(4)−B(5)	1.893(11)
B(4)−B(8)	1.82(1)	B(4)−B(9)	1.77(1)	B(4)−C(21)	1.57(1)	B(5)−B(9)	1.822(11)
B(5)−B(10)	1.83(1)	B(5)−C(31)	1.58(1)	B(6)−B(7)	1.77(1)	B(6)−B(10)	1.759(11)
B(6)−B(11)	1.76(1)	B(7)−B(8)	1.76(1)	B(7)−B(11)	1.75(1)	B(8)−B(9)	1.751(11)
B(8)−B(11)	1.75(1)	B(9)−B(10)	1.80(1)	B(9)−B(11)	1.79(1)	B(10)−B(11)	1.804(11)
C(11)−C(12)	1.34(1)	C(12)−C(13)	1.48(1)	C(13)−C(14)	1.39(2)	C(13)−C(15)	1.549(17)
C(13)−C(16)	1.43(2)	C(21)−C(22)	1.33(1)	C(22)−C(23)	1.53(1)	C(23)−C(24)	1.522(11)
C(23)−C(25)	1.57(1)	C(23)−C(26)	1.50(1)	C(31)−C(32)	1.31(1)	C(32)−C(33)	1.501(11)
C(33)−C(34)	1.52(1)	C(33)−C(35)	1.51(1)	C(33)−C(36)	1.56(1)	C(3)−O(3)	1.150(11)
C(4)−O(4)	1.14(1)	P(1)−C(5)	1.80(1)	P(1)−C(6)	1.79(1)	P(1)−C(7)	1.793(10)

C(1)−Ru(1)−C(2)	43.1(2)	C(1)−Ru(1)−B(3)	77.2(2)	C(2)−Ru(1)−B(3)	44.6(2)	C(1)−Ru(1)−B(4)	78.0(3)
C(2)−Ru(1)−B(4)	76.6(2)	B(3)−Ru(1)−B(4)	47.7(3)	C(1)−Ru(1)−B(5)	45.7(3)	C(2)−Ru(1)−B(5)	76.5(3)
B(3)−Ru(1)−B(5)	81.4(3)	B(4)−Ru(1)−B(5)	48.0(3)	C(1)−Ru(1)−C(3)	162.5(3)	C(2)−Ru(1)−C(3)	120.2(3)
B(3)−Ru(1)−C(3)	85.8(3)	B(4)−Ru(1)−C(3)	93.8(3)	B(5)−Ru(1)−C(3)	136.2(3)	C(1)−Ru(1)−C(4)	108.9(3)
C(2)−Ru(1)−C(4)	151.5(3)	B(3)−Ru(1)−C(4)	152.9(3)	B(4)−Ru(1)−C(4)	106.6(3)	B(5)−Ru(1)−C(4)	84.8(3)
C(3)−Ru(1)−C(4)	88.2(3)	C(1)−Ru(1)−P(1)	97.2(2)	C(2)−Ru(1)−P(1)	91.6(2)	B(3)−Ru(1)−P(1)	119.6(2)
B(4)−Ru(1)−P(1)	167.0(2)	B(5)−Ru(1)−P(1)	135.0(2)	C(3)−Ru(1)−P(1)	87.4(2)	C(4)−Ru(1)−P(1)	86.4(3)
Ru(1)−C(3)−O(3)	178.4(7)	Ru(1)−C(4)−O(4)	178.7(7)	Ru(1)−P(1)−C(5)	116.5(4)	Ru(1)−P(1)−C(6)	116.9(3)
C(5)−P(1)−C(6)	101.7(5)	Ru(1)−P(1)−C(7)	113.9(3)	C(5)−P(1)−C(7)	105.1(5)	C(6)−P(1)−C(7)	100.6(5)
Ru(1)−B(3)−C(11)	111.3(4)	C(2)−B(3)−C(11)	112.0(5)	B(4)−B(3)−C(11)	139.7(6)	B(7)−B(3)−C(11)	108.2(5)
B(8)−B(3)−C(11)	128.1(6)	Ru(1)−B(4)−C(21)	110.9(5)	B(3)−B(4)−C(21)	127.2(6)	B(5)−B(4)−C(21)	120.4(5)
B(8)−B(4)−C(21)	125.9(6)	B(9)−B(4)−C(21)	121.8(6)	Ru(1)−B(5)−C(31)	119.0(5)	C(1)−B(5)−C(31)	133.4(6)
B(4)−B(5)−C(31)	119.6(6)	B(9)−B(5)−C(31)	112.2(6)	B(10)−B(5)−C(31)	115.2(6)	B(3)−C(11)−C(12)	140.6(6)
C(11)−C(12)−C(13)	132.4(7)	C(12)−C(13)−C(14)	109.8(9)	C(12)−C(13)−C(15)	107.0(9)	C(12)−C(13)−C(16)	118.7(7)
C(14)−C(13)−C(15)	107(1)	C(14)−C(13)−C(16)	110(1)	C(15)−C(13)−C(16)	103.6(9)	B(4)−C(21)−C(22)	138.6(7)
C(21)−C(22)−C(23)	136.6(6)	C(22)−C(23)−C(24)	105.3(6)	C(22)−C(23)−C(25)	107.0(6)	C(22)−C(23)−C(26)	116.8(6)
C(24)−C(23)−C(25)	110.2(6)	C(24)−C(23)−C(26)	111.0(6)	C(25)−C(23)−C(26)	106.4(6)	B(5)−C(31)−C(32)	143.9(7)
C(31)−C(32)−C(33)	131.8(7)	C(32)−C(33)−C(34)	110.2(7)	C(32)−C(33)−C(35)	116.0(7)	C(32)−C(33)−C(36)	107.7(7)
C(34)−C(33)−C(35)	108.3(7)	C(34)−C(33)−C(36)	108.0(8)	C(35)−C(33)−C(36)	106.4(7)		

Downloaded by CARLI CONSORTIUM on June 30, 2009
Published on March 19, 1996 on http://pubs.acs.org | doi: 10.1021/om950934+

C(H)=C(H) groups. Cisoid couplings are smaller than transoid ones, but both can occur in the range 12−21 Hz.[5] Significantly, in the spectra of the species **12**, two of the vinyl groups have ^{1}H−^{1}H couplings which are the same while that for the third vinyl group is different. Among the three sets of pairs of peaks we ascribe the pair displaying the smaller ^{1}H−^{1}H coupling (12 Hz for **12a** and 16 Hz for **12b**) to the vinyl group which is coordinated to the ruthenium. In the ^{1}H NMR spectra of **8a** and **10a**, which contain one such C(H)=C(H)R group, the ^{1}H−^{1}H couplings are very similar, being 14 and 16 Hz, respectively. A further feature of the ^{1}H NMR spectra of the compounds **12** is the appreciable difference in chemical shifts for the resonances for the cage CH protons in each complex (δ 2.33 and 4.21 for **12a** and δ 1.71 and 4.43 for **12b**). As discussed above, we ascribe this to an asymmetric structure in which the η^2-coordinated C(H)=C(H)R group is attached to a boron atom adjacent to carbon in the CCBBB ring.

The ^{13}C{^{1}H} NMR spectrum of **12a** shows broad signals at δ 130.2 and 84.8 diagnostic for *C*(H)B nuclei. Similar resonances occur in the spectrum of **12b** at δ 151.4 and 101.9 (Table 2). The resonance at δ 84.8 in the spectrum of **12a** may be assigned to the carbon of the *C*(H)B fragment of the C(H)=C(H)Bu^t group ligating the ruthenium atom, since it corresponds closely in chemical shift to that observed at δ 86.5 for the similar group in the spectra of the isomers **8**. Moreover, the peak at δ 101.9 in the ^{13}C{^{1}H} NMR spectrum of **12b** is very similar to the chemical shift at δ 98.5 for the carbons of the *C*(H)B groups in the spectrum of the isomeric mixture **10**. For **12b** it is also instructive to compare the resonance at δ 79.8 for the *C*(H)SiMe$_3$ nucleus of the C(H)=C(H)SiMe$_3$ group η^2-coordinated to the ruthenium atom with the corresponding signal for this carbon at δ 79.4 in the ^{13}C{^{1}H} NMR spectrum of **10a**.

The NMR spectra of the complexes **12** were all measured at ambient temperatures. Under these conditions the ruthenium atom evidently remains coordinated to one C(H)=C(H)R cage substituent, there being no dissociation so as to allow another vinyl group to adopt an η^2-bonding mode. In this context it was of interest to investigate reactions between the complexes **12** and PMe$_3$. In this manner the complexes [Ru(CO)$_2$(PMe$_3$){η^5-9,10,11-[C(H)=C(H)Bu^t]$_3$-7,8-C$_2$B$_9$H$_8$}] (**13**) and [Ru(CO)$_2${σ,η^5-9-C(H)(PMe$_3$)C(H)SiMe$_3$-10,11-[C(H)=C(H)SiMe$_3$]$_2$-7,8-C$_2$B$_9$H$_8$}] (**14**) were prepared, data for which are given in Tables 1 and 2.

An X-ray diffraction study was carried out on **13**. The significant bond distances and angles are listed in Table 5, and the molecular structure is shown in Figure 3. On one side the Ru atom is coordinated by two CO ligands and the PMe$_3$ molecule, the Ru−P distance (2.359(2) Å) being close to the average found (2.307 Å) in other ruthenium complexes containing this ligand.[14] On the other side, the metal atom is bonded in an η^5 manner to the open face of the cage, with the Ru−C connectivities (2.219(6)−2.226(6) Å) being somewhat shorter than the Ru−B (2.270(8)−2.378(8) Å), as is usual. The three boron atoms of the CCBBB face carry exo-polyhedral C(H)=C(H)Bu^t groups (B−C average 1.58 Å, C=C average 1.33 Å). To our knowledge this is the first molecule to be prepared and to be crystallographically characterized where all the boron atoms in the CCBBB

(14) Orpen, A. G.; Brammer, L.; Allen, F. H.; Kennard, O.; Watson, D. G.; Taylor, R. *J. Chem. Soc., Dalton Trans.* **1989**, S1.

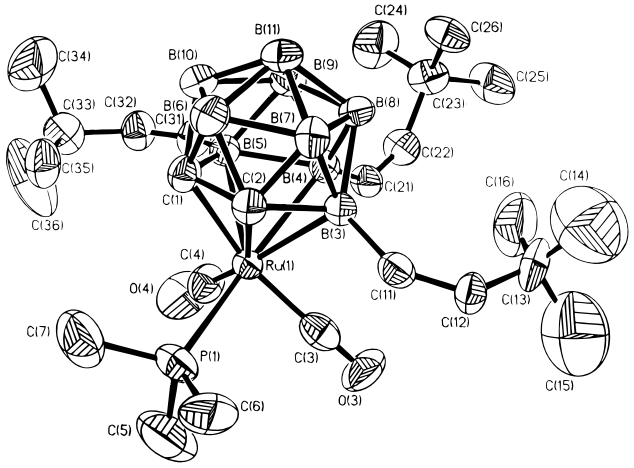

Figure 3. Structure of $[Ru(CO)_2(PMe_3)\{\eta^5\text{-}9,10,11\text{-}[C(H)=C(H)Bu^t]_3\text{-}7,8\text{-}C_2B_9H_8\}]$ (**13**), showing the crystallographic labeling scheme. Hydrogen atoms are omitted for clarity, and thermal ellipsoids are shown at the 50% probability level.

face of a *nido*-C_2B_9 cage system coordinated to a metal have organic groups as substituents.

The NMR data (Table 2) for **13** are in complete agreement with the structure established by the X-ray diffraction study. The *nido* cage fragment is symmetric, with a mirror plane of symmetry through the atoms Ru and B(10) and the mid-point of the cage C−C connectivity. Hence, in the ^1H NMR spectrum the cage CH protons give one signal (δ 2.88) and the protons of the three C(H)=C(H)Bu^t divide into two sets. The doublet signals at δ 5.69 and 6.28, each with a relative intensity corresponding to a single proton, may be assigned to the C(H)=C(H) group at the B(10) or β-site in the CCB*B*B ring, while the doublet signals at δ 5.41 and 5.53, each with relative intensity corresponding to two protons, may be attributed to the C(H)=C(H) groups at the B(9) and B(11) or α-sites in the CC*B*BB ring. The magnitude of the $^1H-^1H$ coupling (16 Hz) between the vinylic protons is at the upper end of the range generally found for a cisoid C(H)=C(H) structure, as found (Figure 3) for all three groups in the crystal structure study. As expected, the resonances for the 27 protons of the Bu^t groups occur as two singlets at δ 1.04 and 1.10 with relative intensity 18:9. The remaining resonance, a doublet at δ 1.67, is due to the PMe_3 ligand. In the $^{31}P\{^1H\}$ NMR spectrum the phosphine group displays a singlet at δ −5.3. In the $^{11}B\{^1H\}$ NMR spectrum the resonances for the three B nuclei carrying C(H)=C(H)Bu^t substituents occur at δ 9.0 and 1.0 and are of relative intensity 1:2, respectively.

In interesting contrast with the formation of **13** by treatment of **12a** with PMe_3, reaction of **12b** with the phosphine yields the ylide complex $[Ru(CO)_2\{\sigma,\eta^5\text{-}9\text{-}C(H)(PMe_3)C(H)SiMe_3\text{-}10,11\text{-}[C(H)=C(H)SiMe_3]_2\text{-}7,8\text{-}C_2B_9H_8\}]$ (**14**). There was no evidence for the formation of an analog of **13**. The data obtained for **14** are in complete agreement with the formulation. The $^{11}B\{^1H\}$ NMR spectrum has three resonances for the B−C(H) groups at δ 3.3, −1.7, and −8.5, and these peaks remain as singlets in fully coupled ^{11}B spectra. In the $^{31}P\{^1H\}$ NMR spectrum the PMe_3 group gives rise to a singlet signal at δ 21.6, a chemical shift similar to that measured for the PMe_2Ph fragment in the $^{31}P\{^1H\}$ NMR spectrum of the ylide compound **11b**. The ^1H NMR spectrum shows all the expected resonances for this asymmetric molecule. There are three peaks for the nonequivalent $SiMe_3$ groups at δ 0.00, 0.03, and 0.19, each of an intensity for nine protons. The resonance for the RuC(*H*)$SiMe_3$ proton occurs as a doublet (δ 1.54, J(HH) = 15 Hz). A doublet resonance at δ 1.63 (J(PH) =13 Hz) may be assigned to the PMe_3 protons. A broad multiplet at δ 2.35 of an intensity corresponding to two protons is assigned to the C*H*PMe_3 proton and the proton of one of the cage CH groups. The resonance for the other cage CH group is seen at δ 3.88. Doublet signals at δ 5.72, 5.89, 6.50, and 6.93, each of an intensity indicating that it was due to a single proton, can be assigned to the two pendant C(H)=C(H) groups. The $^{13}C\{^1H\}$ NMR spectrum was less well resolved, although those peaks observed were as expected.

Conclusions

The results described in this paper demonstrate the considerable versatility of **3a** as a synthon. Further studies on reactions of alkyne complexes of type **5** with nucleophiles merit attention. Complexes **8**−**14** provide novel examples of the nonspectator role of the carborane ligand in half-sandwich systems.[2,15] In complexes **12**−**14** all three boron atoms in the pentagonal ring CCBBB coordinated to the metal atom carry substituents. Formation of such species is without precedent in metallacarborane chemistry. The introduction of functional groups into the 3,1,2-MC_2B_9 framework in the manner described herein suggests new areas for study based on the character of the substituents.

Experimental Section

General Considerations. Solvents were distilled from appropriate drying agents under nitrogen prior to use. Petroleum ether refers to that fraction of boiling point 40−60 °C. All reactions were carried out under an atmosphere of dry nitrogen using Schlenk line techniques. Chromatography columns (*ca*. 15 cm in length and *ca*. 2 cm in diameter) were packed with silica gel (Aldrich, 70−230 mesh), unless otherwise stated. Celite pads for filtration were *ca*. 3 cm thick. The compounds $[Ru(CO)_3(\eta^5\text{-}7,8\text{-}C_2B_9H_{11})]$ (**1**) and $[NEt_4][RuI(CO)_2(\eta^5\text{-}7,8\text{-}C_2B_9H_{11})]$ (**2**) were prepared as previously described,[1] and the reagent $[Ru(CO)_2(THF)(\eta^5\text{-}7,8\text{-}C_2B_9H_{11})]$ (**3a**) was freshly prepared from **2** and $AgBF_4$ in THF and used *in situ* as a CH_2Cl_2 solution. The reagents K[BH(CHMeEt)$_3$] (a 1.0 M solution in THF) and $Me_3SiC{\equiv}CH$ were obtained from the Aldrich Chemical Co., and the purity of the alkyne was checked by NMR spectroscopy. The NMR spectra were recorded at ambient temperatures in CD_2Cl_2, at the following frequencies: ^1H, 360.13 MHz; ^{13}C, 90.56 MHz; ^{31}P, 145.78 MHz; ^{11}B, 115.5 MHz. ^{31}P NMR chemical shifts quoted in the text are positive to high frequency of 85% H_3PO_4 (external).

Synthesis of $[Ru(CO)_2(NMe_3)(\eta^5\text{-}7,8\text{-}C_2B_9H_{11})]$ (3b). Compound **1** (0.20 g, 0.63 mmol) was dissolved in THF (25 mL), and trimethylamine *N*-oxide (0.05 g, 0.63 mmol) was added. After the mixture was stirred at room temperature for 10 min, solvent was removed *in vacuo*. The residue was taken up in CH_2Cl_2 (5 mL) and the solution chromatographed. Elution with CH_2Cl_2−petroleum ether (2:1) removed a broad yellow band. Evaporation of the solvent *in vacuo* and washing the residue with petroleum ether (20 mL) gave yellow microcrystals of $[Ru(CO)_2(NMe_3)(\eta^5\text{-}7,8\text{-}C_2B_9H_{11})]$ (**3b**; 0.16 g).

(15) Jelliss, P. A.; Stone, F. G. A. *J. Organomet. Chem.* **1995**, *500*, 307.

Downloaded by CARLI CONSORTIUM on June 30, 2009
Published on March 19, 1996 on http://pubs.acs.org | doi: 10.1021/om950934+

Downloaded by CARLI CONSORTIUM on June 30, 2009
Published on March 19, 1996 on http://pubs.acs.org | doi: 10.1021/om950934+

Synthesis of [Ru(CO)$_2$(NCMe)(η^5-7,8-C$_2$B$_9$H$_{11}$)] (3c). Compound **2** (0.20 g, 0.36 mmol) in acetonitrile (25 mL) was treated with $AgBF_4$ (0.07 g, 0.36 mmol). After 2 h the solvent was removed *in vacuo*, and the residue treated with CH_2Cl_2 (25 mL) and the extract filtered through a Celite pad. After the volume of solvent was reduced to *ca*. 5 mL, the mixture was chromatographed. Elution with CH_2Cl_2−petroleum ether (1:1) gave a pale yellow fraction which on evaporating the solvent *in vacuo* and washing the residue with petroleum ether (20 mL) yielded yellow microcrystals of [Ru(CO)$_2$(NCMe)(η^5-7,8-C$_2$B$_9$H$_{11}$)] (**3c**; 0.08 g).

Synthesis of [Ru(CO)$_2$(CNBu^t)(η^5-7,8-C$_2$B$_9$H$_{11}$)] (3d). The reagent **3a** was generated *in situ* by treating **2** (0.20 g, 0.36 mmol) with $AgBF_4$ (0.07 g, 0.36 mmol) in THF (25 mL). After the mixture was stirred for 10 min, solvent was removed *in vacuo*, the residue was suspended in CH_2Cl_2 (25 mL), and the mixture was filtered through a Celite pad to remove AgI. The filtrate containing **3a** was then treated with CNBu^t (0.04 mL, 0.36 mmol) and stirred for a further 10 min. Solvent was removed *in vacuo*, the residue was extracted into Et_2O (2 × 15 mL), and the extracts were filtered through a Celite pad. Evaporating the diethyl ether and washing the residue with petroleum ether (20 mL) gave off-white microcrystals of [Ru(CO)$_2$(CNBu^t)(η^5-7,8-C$_2$B$_9$H$_{11}$)] (**3d**; 0.10 g).

Synthesis of [Ru(CO)$_2$(PPh$_3$)(η^5-7,8-C$_2$B$_9$H$_{11}$)] (3e). A CH_2Cl_2 solution of **3a** was generated *in situ* from **2** (0.20 g, 0.36 mmol), as described above, and PPh_3 (0.10 g, 0.36 mmol) was added to the reaction mixture. After the mixture was stirred for 10 min, solvent was reduced in volume (*ca*. 5 mL) and the mixture chromatographed. Elution with CH_2Cl_2−petroleum ether (1:1) gave a yellow fraction, which on removal of solvent *in vacuo* and washing the residue with petroleum ether (20 mL) yielded yellow microcrystals of [Ru(CO)$_2$(PPh$_3$)(η^5-7,8-C$_2$B$_9$H$_{11}$)] (**3e**; 0.14 g).

Synthesis of the Complexes [Ru(CO)$_2$(alkene)(η^5-7,8-C$_2$B$_9$H$_{11}$)]. (i) A CH_2Cl_2 solution of **3a** was generated *in situ* from **2** (0.20 g, 0.36 mmol), as described above, and a steady stream of ethylene was passed through the reaction mixture. After 10 min the ethylene source was removed and the volume of solvent reduced to *ca*. 5 mL. The mixture was then chromatographed, and elution with CH_2Cl_2−petroleum ether (1:1) removed a broad yellow band. Evaporation of solvent *in vacuo* from the eluate and washing the residue with petroleum ether (20 mL) gave yellow microcrystals of [Ru(CO)$_2$(C$_2$H$_4$)(η^5-7,8-C$_2$B$_9$H$_{11}$)] (**4a**; 0.09 g).

(ii) The procedure employed was as for **4a**, except that propylene was bubbled through the reaction mixture instead of ethylene, to give pale yellow microcrystals of [Ru(CO)$_2$(MeCH=CH$_2$)(η^5-7,8-C$_2$B$_9$H$_{11}$)] (**4b**; 0.09 g).

(iii) A CH_2Cl_2 solution of **3a** was prepared from **2** (0.20 g, 0.36 mmol), and the reaction mixture was treated dropwise with vinyltrimethylsilane (0.06 mL, 0.36 mmol). After the mixture was stirred for 10 min, the volume of solvent was reduced *in vacuo* to *ca*. 5 mL and the mixture chromatographed. Elution with CH_2Cl_2−petroleum ether (1:1) gave a very pale yellow fraction, which on removal of solvent and washing of the residue with petroleum ether yielded microcrystals of [Ru(CO)$_2$(Me$_3$SiCH=CH$_2$)(η^5-7,8-C$_2$B$_9$H$_{11}$)] (**4c**; 0.11 g).

(iv) The procedure employed was identical with that for **4c**, except that norbornene (0.04 g, 0.36 mmol) was added to the reaction mixture instead of vinyltrimethylsilane, to yield off-white microcrystals of [Ru(CO)$_2$(C$_7$H$_{10}$)(η^5-7,8-C$_2$B$_9$H$_{11}$)] (**4d**; 0.12 g).

Synthesis of the complexes [Ru(CO)$_2$(alkyne)(η^5-7,8-C$_2$B$_9$H$_{11}$)]. (i) A CH_2Cl_2 solution of **3a** was generated *in situ* from **2** (0.20 g, 0.36 mmol), as described above for **3d**, and treated with 2-butyne (0.015 mL, 0.36 mmol). The reaction was followed by a change in the pattern in the CO region in the IR spectrum and was complete in *ca*. 10 min. The volume of solvent was reduced to *ca*. 5 mL and the mixture chromatographed. Elution with CH_2Cl_2−petroleum ether (1:1) removed a broad pale yellow fraction, which on evaporation of solvent *in vacuo* and washing the residue with petroleum ether (20 mL) gave yellow microcrystals of [Ru(CO)$_2$(MeC≡CMe)(η^5-7,8-C$_2$B$_9$H$_{11}$)] (**5a**; 0.09 g).

(ii) The procedure employed was identical with that for **5a**, except that diphenylacetylene (0.06 g, 0.36 mmol) was used instead of 2-butyne, to give yellow microcrystals of [Ru(CO)$_2$(PhC≡CPh)(η^5-7,8-C$_2$B$_9$H$_{11}$)] (**5b**; 0.11 g).

Reactions of [Ru(CO)$_2$(MeC≡CMe)(η^5-7,8-C$_2$B$_9$H$_{11}$)]. (i) Complex **5a** (0.10 g, 0.29 mmol) was dissolved in Et_2O (20 mL), and a THF solution of K[BH(CHMeEt)$_3$] (0.32 mL, 0.32 mmol) was added dropwise. The course of reaction was followed by spectral changes in the CO region of the IR and appeared complete after stirring for 10 min, at which stage 18-crown-6 (0.08 g, 0.29 mmol) was added to the suspension. Solvent was then removed *in vacuo* and the residue chromatographed on silanized silica gel (70−230 mesh). Elution with CH_2Cl_2−petroleum ether (1:1) removed a narrow red band, which on evaporation of the eluate *in vacuo* and washing of the residue with petroleum ether (20 mL) gave red microcrystals of [K(18-crown-6)][Ru{C(Me)=C(H)Me}(CO)$_2$(η^5-7,8-C$_2$B$_9$H$_{11}$)] (**6**; 0.13 g).

(ii) Complex **5a** (0.10 g, 0.29 mmol) was dissolved in CH_2Cl_2 (20 mL) and PPh_3 (0.08 g, 0.32 mmol) was added. After the mixture was stirred for 1 h, the solvent was reduced in volume to *ca*. 5 mL and the mixture chromatographed. Elution with CH_2Cl_2−THF (5:1) eluted a narrow pale yellow band, which on removal of solvent *in vacuo* and washing of the residue with petroleum ether (20 mL) gave pale yellow microcrystals of [Ru{C(Me)=C(Me)PPh$_3$}(CO)$_2$(η^5-7,8-C$_2$B$_9$H$_{11}$)] (**7**; 0.11 g).

Synthesis of [Ru(CO)$_2$(η^2:η^5-*n*-C(H)=C(H)Bu^t-7,8-C$_2$B$_9$H$_{10}$)] (8). A CH_2Cl_2 solution of **3a** was prepared from **2** (0.20 g, 0.36 mmol), and Bu^{t}C≡CH (0.04 mL, 0.36 mmol) was added. The mixture was stirred for 10 min, after which time the volume of solvent was reduced to *ca*. 5 mL and the solution chromatographed. Elution with CH_2Cl_2−petroleum ether (1:1) removed a broad yellow fraction, which gave, after evaporation of solvent *in vacuo* and washing of the residue with petroleum ether (20 mL), yellow microcrystals of [Ru(CO)$_2$(η^2:η^5-*n*-C(H)=C(H)Bu^t-7,8-C$_2$B$_9$H$_{10}$)] (**8**; 0.09 g). NMR studies showed that the major component (ca 60%) was isomer **8a** and that trace amounts of **12a** were present.

Synthesis of [Ru(CO)$_2$(η^2:η^5-*n*-CH=CH$_2$-7,8-C$_2$B$_9$H$_{10}$)] (9). (i) A solution of **3a** in CH_2Cl_2 was prepared from **2** (0.20 g, 0.36 mmol) and treated with Me$_3$SiC≡CH (0.05 mL, 0.36 mmol). After the mixture was stirred for 10 min, solvent was removed *in vacuo*. The residue was extracted with petroleum ether (2 × 15 mL) and the extracts filtered through a Celite pad. The mixture was then concentrated to a small volume (*ca*. 5 mL) and chromatographed. Elution with CH_2Cl_2−petroleum ether (1:1) removed a single broad pale yellow band, which on evaporation of the solvent *in vacuo* yielded [Ru(CO)$_2$(η^2:η^5-*n*-CH=CH$_2$-7,8-C$_2$B$_9$H$_{10}$)] (**9**; 0.08 g). The product was rechromatographed, with petroleum ether only as eluent, and two separate yellow fractions were thereby isolated, giving after removal of solvent the isomers **9a** and **9b** in a *ca*. 1:4 ratio, as established by ^{1}H NMR measurements.

(ii) A solution of **3a** was prepared *in situ*, as above, and a single pellet of calcium carbide was added to the CH_2Cl_2 solution. Water (5 mL) was added and the mixture stirred for 1 h. Solvent was then removed *in vacuo*, the residue was extracted with petroleum ether (2 × 10 mL), and the extracts were dried over sodium sulfate. After filtration through Celite, solvent was reduced in volume to *ca*. 5 mL. Chromatography with CH_2Cl_2−petroleum ether (1:1) as eluant afforded a single broad pale yellow eluate, which on evaporation of the solvent *in vacuo* yielded [Ru(CO)$_2$(η^2:η^5-n-CH=CH$_2$-7,8-C$_2$B$_9$H$_{10}$)] (**9**; 0.09 g).

Synthesis of the Complexes [Ru(CO)$_2$(η^2:η^5-*n*-C(H)=C(H)SiMe$_3$-7,8-C$_2$B$_9$H$_{10}$)] (10). Compound **3a** was prepared from **2** (0.20 g, 0.36 mmol) as above. After THF was removed

Table 6. Data for X-ray Crystal Structure Analyses[a]

	8a	11b	13
cryst dimens/mm	0.08 × 0.31 × 0.31	0.13 × 0.43 × 0.43	0.25 × 0.28 × 0.31
formula	$C_{10}H_{21}B_9O_2Ru{\cdot}0.125CH_2Cl_2$	$C_{14}H_{25}B_9O_2PRu{\cdot}0.5CH_2Cl_2$	$C_{25}H_{50}B_9O_2PRu$
M_r	371.6	496.1	612.0
cryst color, shape	yellow, irregular	yellow, parallelepiped	colorless, irregular
cryst system	monoclinic	triclinic	monoclinic
space group (No.)	$P2_1/n$ (14)	$P\bar{1}$(2)	$P2_1/n$ (14)
a/Å	6.696(1)	10.213(3)	11.450(2)
b/Å	24.520(5)	10.916(3)	19.545(3)
c/Å	10.262(2)	12.309(3)	15.251(2)
α/deg		101.81(2)	
β/deg	97.79(1)	103.44(2)	90.12(1)
γ/deg		106.53(2)	
V/Å^3	1669.3(5)	1224.3(6)	3413(1)
Z	4	2	4
d_{calcd}/g cm^{-3}	1.479	1.346	1.191
μ(Mo Kα)/cm^{-1}	9.14	8.10	5.16
F(000)/e	744	498	1280
2θ range/deg	3.0−40.0	3.0−40.0	3.0−40.0
no. of rflns measd	1784	2448	3744
no. of unique rflns	1551	2275	3164
no. of obsd rflns	1382	2174	2726
criterion for observn $n(F_o \geq n\sigma(F_o))$	$n = 4$	$n = 4$	$n = 4$
weighting factor g ($w^{-1} = [\sigma^2(F_o) + g\|F_o\|^2]$)	0.0020	0.0096	0.0010
rflns limits			
h	0−6	0−9	0−10
k	0−23	−10 to +10	0−18
l	−9 to +9	−11 to +11	−14 to +14
data−to−param ratio	6.9:1	7.51	7.9:1
R (R')[b]	0.028 (0.037)	0.071 (0.081)	0.049 (0.057)
final electron density diff features (max/min)/e Å^{-3}	+0.35/−0.35	+1.31/−1.29	+1.12/−0.58
S (goodness of fit)	1.11	1.25	1.86

[a] Data collected at room temperature on an Enraf-Nonius CAD4-F automated diffractometer operating in the $\omega-2\theta$ scan mode; graphite-monochromated Mo Kα X-radiation, $\bar{\lambda} = 0.710\ 73$ Å. Refinement was block full-matrix least squares on F, where $\sigma_c^2(F_o)$ is the variance in F_o due to counting statistics. [b] $R = \sum||F_o| - |F_c||/\sum|F_o|$, $R' = \sum w^{1/2}||F_o| - |F_c||/\sum w^{1/2}|F_o|$.

in vacuo and the residue was redissolved in CH_2Cl_2, the filtered solution was concentrated to a small volume (*ca.* 5 mL) and chromatographed. Elution with CH_2Cl_2−THF (5:1) removed a single broad pale yellow band, which on evaporation of the solvent *in vacuo* gave an analytically pure sample of **3a**.[1] This was then redissolved in CH_2Cl_2 (20 mL), $Me_3SiC{\equiv}CH$ (0.05 mL, 0.36 mmol) was added, and the mixture was stirred for 10 min. Solvent was reduced to a small volume (ca. 5 mL), and the mixture was chromatographed on silanized silica gel. Elution with CH_2Cl_2−petroleum ether (1:2) removed a single broad pale yellow band, which on evaporation of solvent *in vacuo* yielded a mixture of **9** and [Ru(CO)$_2$(η^2:η^5-*n*-C(H)═C(H)SiMe$_3$-7,8-$C_2B_9H_{10}$)] (**10**; 0.08 g). From relative peak intensities in the $^{11}B\{^1H\}$ NMR studies it was estimated that the major component was complex **10** (*ca.* 60%) and that the isomers **10a** and **10b** are formed in a ratio of *ca.* 1:4, similar to that of **9**.

Synthesis of [Ru(CO)$_2$(σ,η^5-10-C(H)(PMe$_2$Ph)CH$_2$-7,8-$C_2B_9H_{10}$)] (11b). A sample of **9** was freshly prepared from **3a** (0.36 mmol) and $Me_3SiC{\equiv}CH$, as above. After extraction into heptane (25 mL) the mixture was filtered through a Celite pad, and PMe_2Ph (0.73 mL, 0.36 mmol, 0.5 M solution in THF) was added. Instantaneously a white precipitate formed. The mixture was allowed to settle, and the solvent was decanted off. The resulting white powder was recrystallized from CH_2Cl_2 by addition of petroleum ether, yielding off-white crystals of [Ru(CO)$_2$(σ,η^5-10-C(H)(PMe$_2$Ph)CH$_2$-7,8-$C_2B_9H_{10}$)] (**11b**; 0.10 g).

Synthesis of [Ru(CO)$_2${η^2:η^5-9-C(H)═C(H)Bu^t-10,11-[C(H)═C(H)Bu^t]$_2$-7,8-$C_2B_9H_8$}] (12a). A solution of **3a** in CH_2Cl_2 was prepared from **2** (0.20 g, 0.36 mmol) as above and treated with Bu^{t}C≡CH (0.20 mL, 1.8 mmol). The reaction mixture was stirred for 30 min, after which time the solvent was reduced to a small volume (*ca.* 5 mL) and the mixture chromatographed. Elution with CH_2Cl_2−petroleum ether (1:1) removed a broad yellow fraction, which on evaporation of solvent *in vacuo* yielded yellow microcrystals of [Ru(CO)$_2${η^2:η^5-9-C(H)═C(H)Bu^t-10,11-[C(H)═C(H)Bu^t]$_2$-7,8-$C_2B_9H_8$}] (**12a**; 0.11 g).

Synthesis of [Ru(CO)$_2${η^2:η^5-9-C(H)═C(H)SiMe$_3$-10,11-[C(H)═C(H)SiMe$_3$]$_2$-7,8-$C_2B_9H_8$}] (12b). Complex **3c** (0.10 g, 0.30 mmol) was dissolved in CH_2Cl_2 (20 mL) and $Me_3SiC{\equiv}CH$ (0.21 mL, 1.5 mmol) added. After the reaction mixture was stirred for 15 h, solvent was reduced to *ca.* 5 mL and the mixture chromatographed on silanized silica gel. Elution with CH_2Cl_2−petroleum ether (1:1) removed a single yellow fraction, which on evaporation of solvent *in vacuo* yielded yellow microcrystals of [Ru(CO)$_2${η^2:η^5-9-C(H)═C(H)-SiMe$_3$-10,11-[C(H)═C(H)SiMe$_3$]$_2$-7,8-$C_2B_9H_8$}] (**12b**; 0.09 g).

Synthesis of [Ru(CO)$_2$(PMe$_3$){η^5-9,10,11-[C(H)═C(H)-Bu^t]$_3$-7,8-$C_2B_9H_8$}] (13). Complex **12a** (0.05 g, 0.09 mmol) was dissolved in petroleum ether (20 mL) and PMe_3 (0.09 mL, 0.09 mmol) added. Instantaneous formation of a white precipitate was observed. The mixture was allowed to settle and the solvent decanted. The resulting residue was recrystallized from CH_2Cl_2 by addition of petroleum ether to yield off-white crystals of [Ru(CO)$_2$(PMe$_3$){η^5-9,10,11-[C(H)═C(H)-Bu^t]$_3$-7,8-$C_2B_9H_8$}] (**13**; 0.04 g).

Synthesis of [Ru(CO)$_2${σ,η^5-9-C(H)(PMe$_3$)C(H)SiMe$_3$-10,11-[C(H)═C(H)SiMe$_3$]$_2$-7,8-$C_2B_9H_8$}] (14). Complex **12b** (0.05 g, 0.08 mmol) was dissolved in petroleum ether (20 mL) and treated with PMe_3 (0.08 mL, 0.08 mmol). The mixture was stirred for 10 min, after which time solvent was removed *in vacuo*. The residue was dissolved in CH_2Cl_2 (*ca.* 5 mL) and the solution chromatographed on silanized silica gel. Elution with CH_2Cl_2−petroleum ether (1:1) removed a single yellow fraction, which on evaporation of solvent *in vacuo* yielded yellow microcrystals of [Ru(CO)$_2${σ,η^5-9-C(H)(PMe$_3$)C(H)SiMe$_3$-10,11-[C(H)═C(H)SiMe$_3$]$_2$-7,8-$C_2B_9H_8$}] (**14**; 0.04 g).

Crystal Structure Determinations and Refinements. The crystal and other experimental data for compounds **8a**, **11b** and **13** are listed in Table 6. Diffraction-quality crystals were grown from CH_2Cl_2−petroleum ether solutions and selected on the basis of optical homogeneity. Final lattice

Downloaded by CARLI CONSORTIUM on June 30, 2009
Published on March 19, 1996 on http://pubs.acs.org | doi: 10.1021/om950934+

parameters were obtained at high θ angles, >20°. Data were collected at varied scan speeds in ω of 0.56−5.17° min^{-1} for **8a,** 0.69−5.17° min^{-1} for **11b**, and 0.54−5.17° min^{-1} for **13** with respective scan ranges of 1.15, 1.25, and 1.15° + 0.34 tan θ. No significant variations were observed in the intensities of the monitored check reflections for **8a** and **13** (every 2 h, <1.2%). However, for **11b**, an average decay of −0.3% h^{-1} was rectified using the program DECAY[16] (maximum correction 1.107 20). After removal of check intensity reflections from each data set, averaging of duplicate and equivalent data was carried out. The remaining intensity data were corrected for Lorentz and polarization effects, after which an empirical absorption correction[16] based on high-angle Ψ scans was performed on **8a** and **13** (transmission factors: minimum, 0.9104 and 0.9148; maximum, 0.9996 and 0.9996, respectively), and a numerical absorption correction based on crystal face measurements was performed on **11b** (transmission factors: minimum, 0.6981; maximum, 0.9163). After the zero moment test (NZ test)[17] was applied to the observed data sets, centrosymmetric systems were indicated for all compounds of interest.

The structure solutions for **8a** and **13** were obtained by the Patterson technique,[18] which rendered all non-hydrogen atom positions. For **11b**, direct methods[18] yielded the atomic positions of Ru, P, 7 B, and 10 C atoms and the remaining non-hydrogen atoms were located by using standard difference mapping. All hydrogen atoms for compound **8a** were located by density mapping and were allowed to ride on their parent carbon and boron atoms with fixed isotropic thermal parameters (U_{iso} = 80 × 10^{-3} and 60 × 10^{-3} Å^2, respectively). For compounds **11b** and **13**, the cage hydrogen atoms were found using the BHGEN program.[19] In compound **11b**, hydrogen atoms H(3a), H(4a), and H(4b) were located by difference Fourier mapping. All other hydrogen atoms in compounds **11b** and **13** were generated with idealized geometry. All were constrained to ride on their connected carbon and boron atoms with fixed isotropic thermal factors (U_{iso} = 80 × $10^{-3}$and 60 × 10^{-3} Å^2, respectively). The block full-matrix least-squares method[17] was used to refine the models ($P2_1/n$ for **8a** and **13**, $P\bar{1}$ *for* **11b**) and 200, 290, and 344 parameters were respectively refined using the minimized quantity $\sum w(||F_o| - |F_c||)^2$. Final Fourier difference maps revealed some density in the vicinity of the heavy-metal atoms; elsewhere, the maps were featureless with only random fluctuating background. Atomic scattering factors were taken from the usual source.[20]

Acknowledgment. We thank the Robert A. Welch Foundation for support (Grants AA-1201 and -0668).

Supporting Information Available: Complete tables of atomic coordinates, bond lengths and angles, anisotropic thermal parameters and hydrogen atom parameters for **8a**, **11b**, and **13** (26 pages). Ordering information is given on any current masthead page.

OM950934+

(16) Enraf-Nonius Vax Structure Determination Package; Enraf-Nonius, Delft, The Netherlands, 1989.
(17) Howells, E. R.; Phillips, D. C.; Rogers, D. *Acta Crystallogr.* **1950**, *3*, 210.
(18) Siemens SHELXTL-PC; Siemens X-ray Instruments; Madison, WI, 1989.
(19) Sherwood, P. BHGEN, a Program for the Calculation of Idealized Hydrogen-Atom Positions for a *nido*-Icosahedral Carbaborane Fragment; Bristol, University, U.K., 1986.
(20) *International Tables for X-ray Crystallography;* Kynoch Press: Birmingham, U.K., 1974; Vol. 4.

Downloaded by CARLI CONSORTIUM on June 30, 2009
Published on March 19, 1996 on http://pubs.acs.org | doi: 10.1021/om950934+